POLITEHNICA UNIVERSITY OF BUCHAREST
DOCTORAL SCHOOL OF MATERIALS SCIENCE AND ENGINEERING

PHD THESIS SUMMARY

STUDIES AND RESEARCH ON THE OBTAINING OF COMPLEX CONCENTRATED ALLOYS WITH REDUCED DENSITY

Author: Drd. Eng. Ioana-Cristina BĂNICĂ (BADEA)
PhD supervisor: Prof. Dr. Eng. Nicolae CONSTANTIN

DOCTORAL COMMITTEE			
President	Prof. dr. Eng. Radu ȘTEFĂNOIU	from	POLITEHNICA University of Bucharest
Phd supervisor	Prof. dr. Eng. Nicolae CONSTANTIN	from	POLITEHNICA University of Bucharest
Referee	Conf. dr. Eng. Erika Diana ARDELEAN	from	POLITEHNICA University of Timișoara
Referee	Prof. dr. Eng. Vasile BRATU	from	VALAHIA University of Târgoviște
Referee	Prof. dr. Eng. Valeriu Gabriel GHICA	from	POLITEHNICA University of Bucharest

BUCHAREST
2023

CONTENT of the PhD thesis

Foreword..... 1
List of tables from the PhD thesis..... 3
List of figures from the PhD thesis..... 4
The project of the scientific research program for the completing the PhD thesis with the title: `Studies and researches on the obtaining of complex concentrated alloys with reduced density`..... 9
Introduction..... 10
PART I: DOCUMENTARY ANALYSIS OF THE CURRENT STATE OF PRODUCTION AND USE OF LOW DENSITY COMPLEX CONCENTRATED ALLOYS
CHAPTER 1. General presentation of complex concentrated alloys..... 13
1.1. Retrospective on multicomponent alloys..... 13
1.2. Definitions of multicomponent alloys..... 14
1.3. Characteristics of multicomponent alloys..... 16
CHAPTER 2. Phase selection in multicomponent alloy systems..... 21
2.1. Entropy..... 21
2.2. Gibbs`s Law..... 22
2.3. Hume-Rothery rules and thermodynamic parameters for multicomponent alloys..... 23
2.4. Correlations using δ, χ, VEC, ΔH_{mix} and Ω..... 24
2.5. CALPHAD (CALculation of PHAse Diagrams) 26
CHAPTER 3. Classification of complex concentrated alloys..... 28
3.1. CCAs from 3d transition metals..... 28
3.2. Refractory metallic CCAs..... 29
3.3. Other alloy families..... 30
CHAPTER 4. The properties of complex concentrated alloys..... 32
4.1. Functional properties..... 32
4.1.1. Thermal properties..... 32
4.1.2. Electric properties 34
4.1.3. Magnetic properties..... 35
4.2. Mechanical properties..... 36
4.2.1. Hardness and compressive strength 36
4.2.2. Tensile strength 38
4.2.3. Mechanisms of increasing the alloys strength 39
4.2.4. Other mechanical properties..... 40
4.2.5. Refractory CCAs..... 40
4.3. Corrosion properties..... 41
CHAPTER 5. Applications of complex concentrated alloys..... 45
PART II OWN EXPERIMENTAL RESEARCH ON OBTAINING AND CHARACTERIZING LOW DENSITY COMPLEX CONCENTRATED ALLOYS
CHAPTER 6. Materials selection and complex concentrated alloys design..... 50
6.1. The influence of alloying elements on the properties of complex concentrated alloys..... 50
6.2. Selection of low density complex concentrated alloy systems..... 54
6.3. Modelling CCAs structure depending of each element concentration..... 64
6.4. Thermodynamic and Kinetic Simulation of Complex Concentrated Alloys... 67
6.5. Modelling heat treatment and precipitation processes..... 77
6.6. Precipitation kinetics during rapid solidification process..... 80
CHAPTER 7. Synthesis and processing of complex concentrated alloys..... 82

7.1. Elaboration – casting of alloy ingots..... 82
7.2. Heat treatment of elaborated alloys…..... 85
7.3. Obtaining alloy strips through the rapid solidification process..... 91
CHAPTER 8. Characterization of complex concentrated alloys obtained by processing in the induction furnace..... 95
8.1. Chemical characterization..... 95
8.2. Microstructural characterizations..... 96
8.2.1 Optical microscopy characterization…..... 96
8.2.2. Characterization by scanning electron microscopy and energy dispersive spectrometry SEM -EDS……..... 99
8.2.3 Characterization by X-ray diffraction..... 107
8.2.4. Mechanical tests..... 111
8.3. Thermo – physical characterisations..... 115
CHAPTER 9. Characteristics of CCA alloy heat treated by quenching and aging..... 118
9.1. Optical microscopy characterization…..... 118
9.2. Characterization by scanning electron microscopy and energy dispersive spectrometry SEM -EDS……..... 119
9.3. X-ray diffraction characterization of quenched and aged alloy…….... 124
9.4. Microhardness of quenched and aged alloy..... 125
CHAPTER 10. Structural characterizations of the samples obtained through the rapid solidification process..... 126
10.1. Optical microscopy characterisation of CCAs ribbons…..... 126
10.2. Characterization of alloy bands by scanning electron microscopy and SEM-EDS energy dispersive spectrometry…….... 131
10.3. Characterization of alloy ribbons by X-ray diffraction..... 139
CHAPTER 11. Corrosion resistance of $Al_5Cu_{0.5}Si_{0.2}Zn_{1.5}Mg_{0.2}$ alloy……..... 142
CHAPTER 12. The analysis of modelling and experimental results…..... 148
CHAPTER 13.Final conclusions, original contributions and future research directions 154
13.1. Final summary conclusions..... 154
13.2. Personal, original contributions..... 157
13.3. Future directions for the development of doctoral thesis research..... 158
DISSEMINATION OF THE RESULTS FROM THE DOCTORAL THESIS..... 159
REFFERENCES…..... 164

PART I DOCUMENTARY ANALYSIS OF THE CURRENT STATE OF PRODUCTION AND USE OF LOW DENSITY COMPLEX CONCENTRATED ALLOYS

Introduction

Complex concentrated alloys represent a new category of advanced metallic materials that offer a wide spectrum of mechanical and physical characteristics. They are different from conventional alloys because they are based on a high number of main elements and have distinct strategies of obtaining. The properties of complex concentrated alloys offer a high potential for use in various industrial applications, such as: aerospace, marine, medical or machine building. To be effective during use, complex alloys must possess good resistance to oxidation and corrosion, low density, or high hardness.

In the first chapter of the doctoral thesis, a retrospective analysis of multicomponent alloys is performed. The evolution of metallic materials throughout the historical eras, the main advantages and benefits of the integration of metallic materials in daily activities, but also the main challenges of today's society and the need to reduce material and energy consumption, as well as the costs of obtaining, are taken into account.

The second chapter presents the selection process of the constituent elements in complex alloy systems, by using modern thermodynamic and kinetic modeling tools in the formation of specific structures. Also, an analysis is made regarding the correlation of the main alloys compositions systems currently used with their properties and their destinations.

In chapter III and IV complex concentrated alloys are classified, according to the constituent elements and the families they belong to. Also, the main properties of the new materials are presented, which include functional, thermal, electrical, magnetic or mechanical properties, as well as corrosion resistance. The design of these features is done according to their main destinations.

The Vth chapter summarizes the main applications of complex concentrated alloys, as well as their related properties, where the main strategies for the formation of specific structures are also considered.

In Chapter VI, the process of material selection and design of CCA type alloys is presented. The alloying elements have a major impact on the properties of the new materials, and the process of modeling their structure is essential in determining the most suitable compositions and reducing the costs related to the obtaining processes.

Chapter VII presents the synthesis and processing of complex alloys, by analyzing the main methods of elaboration, but also the benefits that the different types of thermal treatments application has on the final structure.

Chapters VIII and IX show the results obtained following the characterization processes of complex concentrated alloys in cast and thermally treated state, using chemical, microstructural and thermophysical analysis techniques.

The Xth chapter presents the main characteristics of the rapid solidification processes and the experimental results obtained by optical, scanning electron and X-ray diffraction microscopy.

Chapter XI includes corrosion resistance tests of newly obtained complex concentrated alloys, as well as certain correlations regarding the analysis of experimental results and those obtained from modeling processes.

The PhD thesis can bring new perspectives on the complex concentrated alloys modeling and obtaining, due to the original contributions, both in the scientific and in the applied plan.

CHAPTER 1. General presentation of complex concentrated alloys

1.2. Definitions of multicomponent alloys

The concept of high-entropy alloys is closely related to obtaining a unique solid solution, with configurational entropy control as the main tool. This causes much controversy and distracts from the main goal of exploring the large number of alloys existent in the vast compositional space. There are several names that suggest the complexity of the compositional space without any meaning regarding the magnitude of the entropy or the types of phases present. These names include multiple principal element alloys (MPEAs) and complex concentrated alloys (CCAs) [1].

Since complex concentrated alloys do not contain a single main element, the sequence of elements entering the composition of the alloy could be presented in different ways. One of the most used methods of effectively comparing alloys within the same system or alloys belonging to different systems is to note the concentration in the form of an atomic ratio or an atomic percentage (as an index of each element in the composition). Also, the indices in the alloy formula can also indicate the mole fraction of the element, where 1 represents the equal mole fraction of the elements [1].

1.3. Characteristics of multicomponent alloys

The basis of the first MPEA publications was the broad category of new alloys and alloy systems offered by the inner regions of the phase diagrams of the multiple principal elements [2,3,4]. This has provided multiple opportunities for the discovery of new alloys with strong scientific and practical value.

Recently, there has been a call for the development of multiphase CCAs with microstructures that can confer excellent structural properties at high temperatures [5,6]. Alloy development is usually based on microstructures with at least one solid solution phase, but recent studies suggest that microstructures consisting of two intermetallic phases can also provide a balance of structural properties if sufficient attention is paid to microstructure control [7]. An area of future focus includes the investigation of multiphase microstructures occurring in CCAs.

Three of the four basic effects, developed and defined by Yeh [8] are high entropy, severe network distortion and slow diffusion, and the fourth effect, proposed by Ranganataha [4], is the cocktail effect. From a thermodynamic point of view, the high entropy effect could affect the formation of complex phases. For kinetics, the slow diffusion effect could slow down the phase transformation. From the structure perspective, the effect of severe lattice distortion could modify the properties. For properties, the cocktail effect brings a surplus to the predicted mixing amounts, usually due to mutual interactions between different atoms and severe lattice distortions [9].

CHAPTER 2. Phase selection in multicomponent alloy systems

2.1. Entropy

The statistical-mechanical definition of entropy was developed by Ludwig Boltzmann in the 1870s by analyzing the statistical behavior of the system microscopic components. Boltzmann's hypothesis states that the entropy of a system is linearly related to the logarithm of the macro-state occurrence frequency or, more precisely, the number, W, of possible micro-states corresponding to the macroscopic state of a system [10]:

$$S = k\, lnW \quad ; \tag{2.1.}$$

where k = 1,38 x 10^{-23} J/K is Boltzmann's constant, and the logarithm is considered the natural base, ``e".

For a more effective prediction of the phases number in a multicomponent alloy, the phase rule proposed by Josiah Willard Gibbs in the 1870s can be applied [11].

2.2. Gibbs's Law

Gibbs' rule refers to the number of phases, P, that a multicomponent system has in thermodynamic equilibrium, to the degrees of freedom, F, (the number of variables that can be changed arbitrarily and independently without changing the equilibrium), and the number of components, N. At constant pressure, Gibbs' phase law is:

$$P = N - F + 1 \quad (2.2.)$$

The phase law limits the number of possible phases and specifies the number of freedom degrees that exist for a given number of phases and components. However, this law does not provide information about how many phases are actually present in any given alloy or system at given values of temperature and pressure. In a system with N components there can be any number of phases, from minimum (1) to maximum (N+1), without breaking Gibbs' theorem [1].

2.3. Hume-Rothery rules and thermodynamic parameters for multicomponent alloys

The Hume-Rothery rules represent the oldest guide in obtaining alloys based on solid solutions [12,13,14]. These rules state that the formation of solid solutions occurs predominantly in alloys whose elements have similar atomic sizes, crystal structures, electronegativities, and valences.

To apply these concepts for the purpose of predicting the formation of the solid-solution phase in complex alloys, the HEA community has developed new relations for atomic radius differences δ, relative electronegativity χ and for the average valence electron concentration (VEC) [15,16]. Thermodynamic considerations are reflected by the mixing enthalpy ΔHam and a parameter Ω that includes ΔH_{mix}, the entropy of mixing ΔS_{mix} and the melting temperature, Tm [17].

Senkov and Miracle propose a simple thermodynamic criterion to predict the intermetallic phase equilibrium presence or absence in a high-entropy alloy at a given temperature T. The ratio k_1 is the ratio of the formation enthalpy of intermetallic compounds to the formation enthalpy of solid solutions, and to form mainly solid solutions it must be lower than a critical value k_1^{cr}.

$$k_1 = \frac{\Delta H_{IM}}{\Delta H_{mix}} < -\frac{T_{trat}\Delta S_{mix}}{\Delta H_{mix}}(1 - k_2) + 1 \equiv k_1^{cr}(T) \quad (2.3.)$$

$$k_2 = \frac{\Delta S_{IM}}{\Delta S_{mix}} \quad (2.4.)$$

ΔH_{IM} - formation enthalpy of intermetallic compounds, J;

ΔS_{am} - formation enthalpy of solid solutions, J/K;

ΔH_{am} - formation enthalpy of solid solutions, J;

ΔS_{IM} - formation enthalpy of intermetallic compounds, J/K;

T_{trat} - homogenization temperature of the alloy structure, K [18].

2.5. CALPHAD (CALculation of PHAse Diagrams)

All packages of thermodynamic programs include thermodynamic databases, which are developed based on the so-called CALPHAD (CALculation of PHAse Diagram) method [19]. The CALPHAD method presents the development of thermodynamic functions that correspond to experimental data from binary and ternary phase diagrams. Quaternary and higher order systems are not used because higher order interactions become so weak that they can be

considered negligible [20] but in terms of using complex alloys it is possible by combining and exploring binary and ternary data [21].

CHAPTER 3. Classification of complex concentrated alloys

The main families of complex concentrated alloys

Complex concentrated alloys can be classified into seven families. These families include 3d transition metal CCAs, refractory metal CCAs, light metal CCAs, transition metal-lanthanide (4f) CCAs, CCA brasses and bronzes, precious metals CCAs and from interstitial compounds CCAs (boride, carbide and nitride) [22].

PART II OWN EXPERIMENTAL RESEARCH ON OBTAINING AND CHARACTERIZING LOW DENSITY COMPLEX CONCENTRATED ALLOYS

CHAPTER 6. Materials selection and complex concentrated alloys design

6.1. The influence of alloying elements on the properties of complex concentrated alloys

In order to determine the most suitable alloy compositions to record superior characteristics in multiple applications, the challenges to which the materials are subjected during operation were analyzed. The main important factor in material selection is density, which has a considerable impact on reducing vehicle fuel consumption while also reducing environmental impact. Another aspect in the choice of the right material is represented by the corrosion resistance, since the degradation of the components through corrosion involves huge financial costs for the industrial economic field. Among other characteristics that materials used in industrial sectors must satisfy shall be listed fracture resistance, yield strength and high temperatures resistance [23].

Analyzing the periodic table of elements, the possible elements that the alloy system can contain were studied, taking into account the ratio between density, corrosion resistance, cost and reactivity.

6.2. Selection of low density complex concentrated alloy systems

From the list of elements mentioned and described previously, those that fall within the required density range are: aluminum, magnesium, titanium, silicon, vanadium, copper, chromium, manganese, nickel, and zinc.

Starting from the selected elements, a modeling was carried out using the Metalmix program, based on the thermodynamic and structural criteria presented in the specialized literature and the scientific community in the field. Metalmix is a modeling program developed within the IMNR and represents a proper calculation software for the criteria of complex concentrated alloys. The program offers the possibility of sorting the obtained results, depending on the order chosen by the operator.

The four alloys selected to be experimentally obtained are $Al_5Cu_{0,5}Si_{0,2}Zn_{1,5}Mg_{0,2}$, $Al_{3,4}Cu_{0,5}Si_{0,2}Zn_{0,5}Mg$, $Al_3Mn_{0,2}Si_{0,8}Zn_{0,3}Mg_{0,7}$ and $Al_4Mn_{0,3}SiZn_{0,3}Mg$.

6.4. Thermodynamic and Kinetic Simulation of Complex Concentrated Alloys

The phase diagram of the $Al_{3,4}Cu_{0,5}Si_{0,2}Zn_{0,5}Mg$ alloy (Fig. 6.1.) made with the MatCalc program indicates two different regions regarding the formation of hard intermetallic phases. The phases based on Zn_2Mg and Al_2Cu are found in higher proportions below the 316°C

temperature and decrease significantly when this temperature is exceeded. The presence of these compounds is determined by the high proportions of Zn, Mg and Cu.

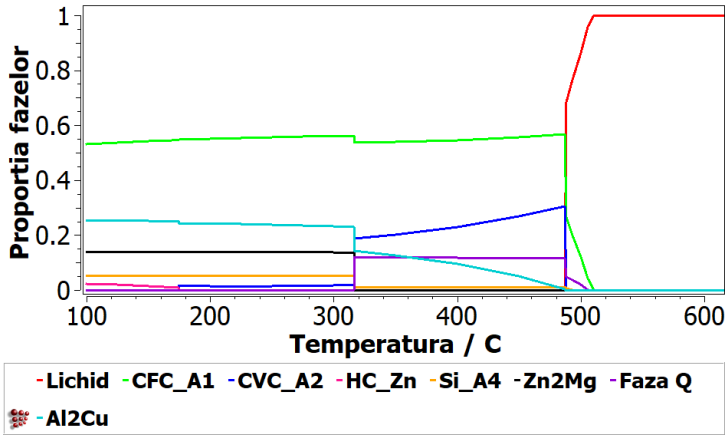

Figure 6.1. The component phases evolution of the $Al_{3,4}Cu_{0,5}Si_{0,2}Zn_{0,5}Mg$ alloy depending on temperature

The results of thermodynamic simulation for the $Al_5Cu_{0,5}Si_{0,2}Zn_{1,5}Mg_{0,2}$ alloy is presented in fig. 6.2 and indicates a predominant presence of solid solutions (CFC-A1 and CVC-A2) in the alloy structure. The Al_2Cu intermetallic phase is also present in considerable proportion at low temperatures. Other intermetallic phases (Zn_2Mg and Mg_2Si) are also identified in the phase diagram, but in minor proportions [24].

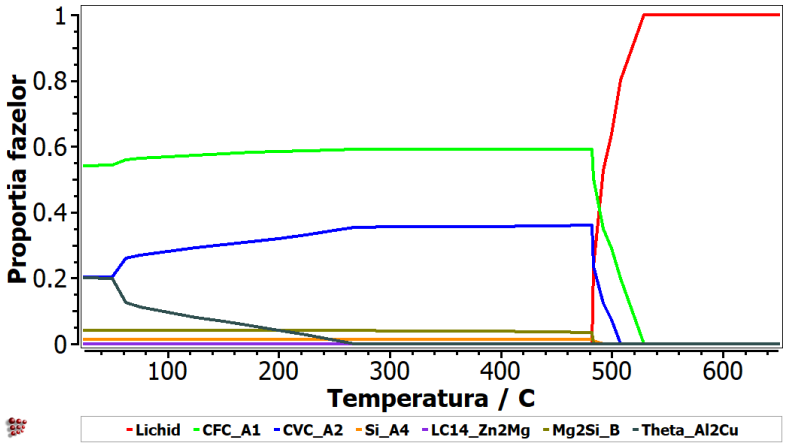

Figure 6.2. The component phases evolution of the $Al_5Cu_{0,5}Si_{0,2}Zn_{1,5}Mg_{0,2}$ alloy depending on temperature

In the $Al_3Mn_{0,2}Si_{0,8}Zn_{0,3}Mg_{0,7}$ alloy phase equilibrium diagram (Fig. 6.3.), two intermetallic phases of the alpha-Al_9Mn_2Si and Mg_2Si type can be observed. They have high stability at low and high temperatures and form early during the solidification process. As in the previous alloy structure, the CFC_A1 phase is predominant at all temperatures, but starts to form after the intermetallic phases [25].

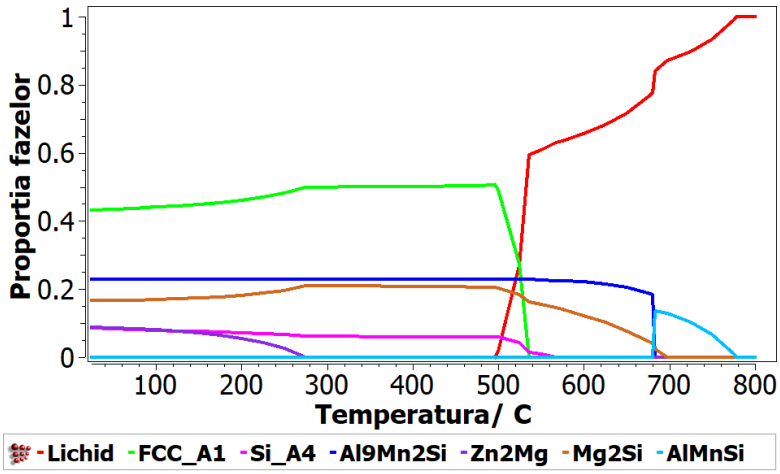

Figure 6.3. The $Al_3Mn_{0,2}Si_{0,8}Zn_{0,3}Mg_{0,7}$ alloy component phases evolution depending on temperature

The phase equilibrium diagram of the $Al_4Mn_{0,3}SiZn_{0,3}Mg$ alloy is represented in fig. 6.4. MatCalc simulation of the phase evolution of alloy component as a function of temperature identified the AlCrFeMnSi phase which has a composition close to the Al_9Mn_2Si phase. This phase together with the Mg_2Si intermetallic phase is found in a high proportion both at low and high temperature values. In contrast, solid solution CFC_A1 exhibits high stability at temperatures up to 500°C after which it drops sharply. The intermetallic compounds Zn_2Mg and Mg_2Zn are present in small proportions at low temperatures.

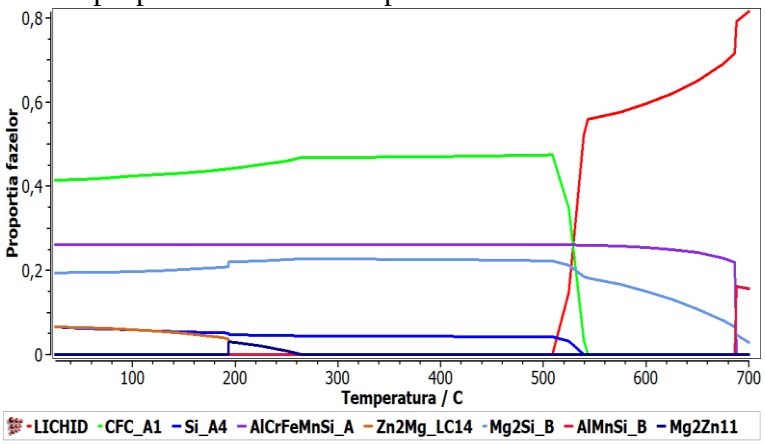

Figure 6.4. The $Al_4Mn_{0,3}SiZn_{0,3}Mg$ alloy component phase evolution depending on temperature

CHAPTER 7. Synthesis and processing of complex concentrated alloys

7.1. Elaboration - casting of alloy ingots

The alloys were melted in the induction furnace type Linn MFG-30 within the National Institute of Research - Development for Non-Ferrous and Rare Metals (INCDMNR - IMNR).

The major steps in the fabrication process in the induction furnace are decrease the pressure until vacuum level, degassing the charge and melting the alloy. In the stage of emptying the premises, the aim is to eliminate impurity gases from the furnace premises and the humidity of the raw materials. After stabilizing the pressure in the furnace, during the melting stage, the temperature of the charge is raised to the melting point and maintained until all materials are dissolved in the melt. The resulting melt is poured into a copper or graphite shell, in a protective atmosphere. After cooling the alloy in the furnace, the CCA ingot is obtained. The next step consists of the heat treatment processes applied to resulted CCA alloys.

7.2. Heat treatment of elaborated alloys

The heat treatments were carried out in the Nabertherm furnace, within the National Institute of Research - Development for Non-Ferrous and Rare Metals (INCDMNR - IMNR), under a protective argon (Ar) atmosphere.

Considering the criterion of the specificity of transformations in the solid state, for the alloys studied in this work, three types of thermal treatments were performed: homogenization annealing treatment and quenching and artificial aging.

The aim of the homogenization treatment is to age the dendritic structure that resulted from the casting and obtain a homogeneous phase that leads to obtaining the desired mechanical characteristics.

7.3. Obtaining alloy strips through the rapid solidification process

The rapid solidification of the $Al_5Cu_{0,5}Si_{0,2}Zn_{1,5}Mg_{0,2}$ alloy was performed using the experimental facility within the National Institute for Research - Development for Non-Ferrous and Rare Metals (INCDMNR - IMNR).

Following the application of the rapid solidification process, alloy ribbons ($Al_5Cu_{0,5}Si_{0,2}Zn_{1,5}Mg_{0,2}$) are obtained at different disc rotations (500 rpm, 1000 rpm and 1500 rpm) and at different distances between the crucible and the disc (0.5mm ,1mm and 1.5mm).

CHAPTER 8. Characterization of complex concentrated alloys obtained by processing in the induction furnace

8.1. Chemical characterization

Each element composition of the analyzed samples is within a maximum of 2 wt.% from the nominal values (table 8.1.). Due to the high percentage of elements, a variation of 2 wt.% in the composition has a weak influence on the structural behavior of the alloys [25].

Table 8.1. Alloys chemical composition on weight percent

Alloy	Type	Al	Mn	Cu	Si	Zn	Mg	Total
$Al_{3.4}Cu_{0.5}Si_{0.2}Zn_{0.5}Mg_{0.2}$	Nominal	55.03	-	19.06	3.37	19.62	2.92	100
	determined	53.6	-	17.8	4.2	20.9	3.2	100
$Al_5Cu_{0.5}Si_{0.2}Zn_{1.5}Mg_{0.2}$	Nominal	49.00	-	11.55	2	35.60	1.80	100
	determined	45.48	-	11.49	2.08	38.87	2.05	100
$Al_3Mn_{0.2}Si_{0.8}Zn_{0.3}Mg_{0.7}$	Nominal	53.59	7.28	-	14.87	12.99	11.27	100
	determined	53.4	8.4	-	15.5	11.6	10.8	100
$Al_4Mn_{0.3}SiZn_{0.3}Mg$	Nominal	54.95	8.39	-	14.29	10.00	12.37	100
	determined	51.25	6.55	-	17.94	12.66	11.6	100

8.2. Microstructural characterizations

8.2.2. Characterization by scanning electron microscopy and energy dispersive spectrometry SEM -EDS

Characterizations by scanning electron microscopy (Fig. 8.1.), highlighted major differences between cast and heat-treated alloys. The alloy $Al_{3.4}Cu_{0.5}Si_{0.2}Zn_{0.5}Mg_{0.2}$ in the as-cast state (Fig. 8.5.a)) consists of similar sizes phases, uniformly distributed in the material. After applying the heat treatment, the alloy shows a large dendritic structure and a well-defined interdendritic eutectic (Fig.8.5. b)) [25].

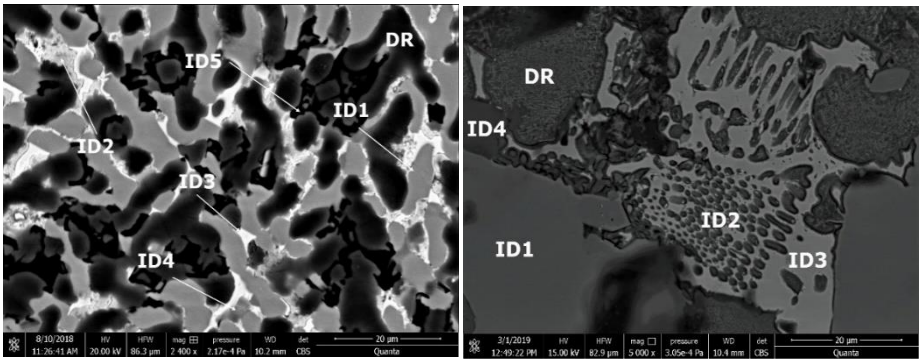

a) b)

Figure 8.1. SEM images of a) as-cast and b) annealed $Al_{3,4}Cu_{0,5}Si_{0,2}Zn_{0,5}Mg_{0,2}$ alloy. DR-dendritic area, ID-interdendritic area.

The $Al_5Cu_{0.5}Si_{0.2}Zn_{1.5}Mg_{0.2}$ alloy in the as-cast state (Fig. 8.2. a)) was characterized by multiple phases homogeneously arranged in the material. As a result of the heat treatment, it can be noted the presence of a large area with a dendritic structure and another smaller area where clearly are defined predominate eutectic structures (Fig. 8.2.b)).

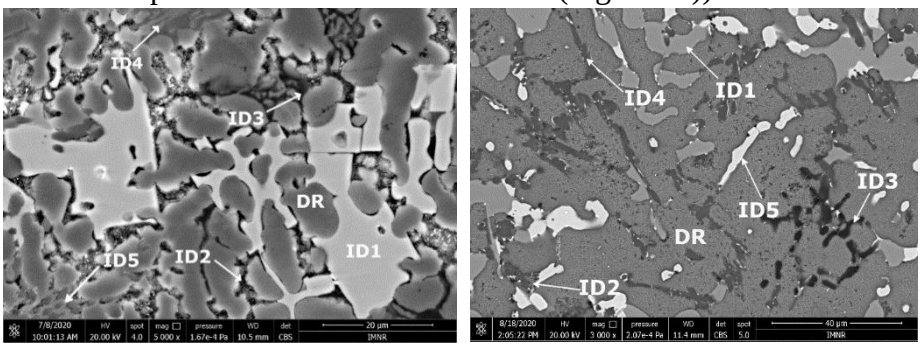

a) b)

Figure 8.2. SEM images of a) as-cast and b) annealed $Al_5Cu_{0.5}Si_{0.2}Zn_{1.5}Mg_{0.2}$ alloy. DR-dendritic area, ID-interdendritic area.

The as-cast and annealed structures for the $Al_3Mn_{0.2}Si_{0.8}Zn_{0.3}Mg_{0.7}$ alloy (Fig.8.3.) look similar with small differences related to the interdendritic distribution of the eutectic phases. Dark intermetallic phases with a dendritic appearance are well distinguished at high magnifications, showing small internal cracks in the annealed sample.

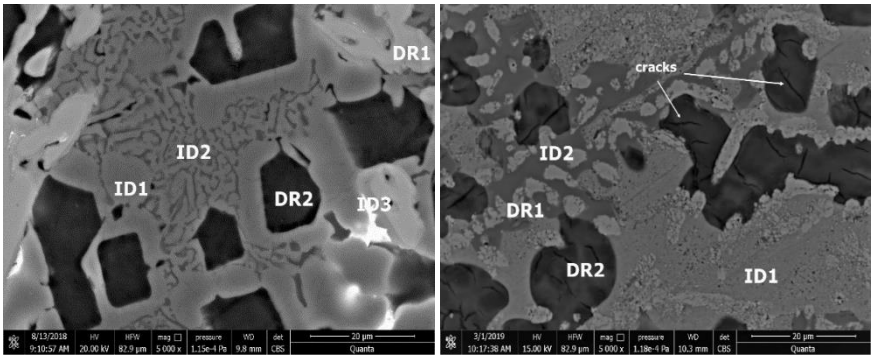

a) b)

Figure 8.3. SEM images of a) as-cast and b) annealed $Al_3Mn_{0.2}Si_{0.8}Zn_{0.3}Mg_{0.7}$ alloy. DR-dendritic area, ID-interdendritic area.

The $Al_4Mn_{0.3}SiZn_{0.3}Mg$ alloy in the as-cast and in the annealed states (Fig. 8.4.) shows multiple phases. The cast alloy shows a typical dendritic morphology. In the area of

interdendritic segregation, the presence of three phases is found, two of which are found in the platelets form and the other has an irregular shape. These three phases are trapped in a matrix formed by a Chinese script type eutectic.

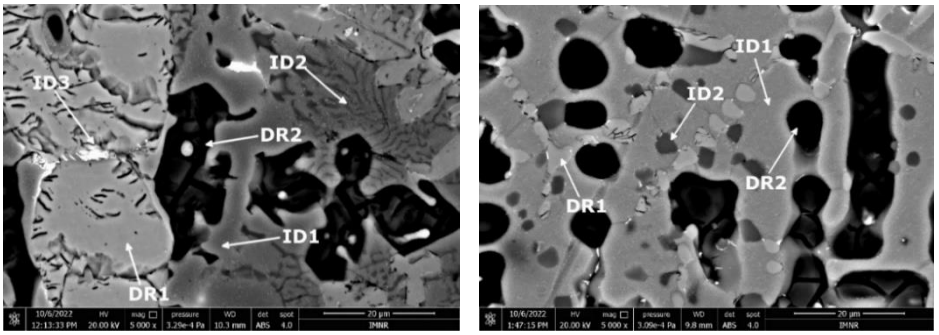

a) b)

Figure 8.4. SEM images of a) as-cast and b) annealed $Al_4Mn_{0.3}SiZn_{0.3}Mg$ alloy. DR-dendritic area, ID-interdendritic area.

8.2.3 Characterization by X-ray diffraction

X-ray analysis of the as-cast $Al_{3.4}Cu_{0.5}Si_{0.2}Zn_{0.5}Mg_{0.2}$ alloy (Fig. 8.5.) indicates a structure composed of solid solutions based on Al and Zn and intermetallic compounds-based phases Al_2Cu, Mg_2Zn_{11}, Mg_2Si, $MgZn_2$.

After the heat treatment performed at 400 ºC for 20 hours (Fig. 8.6.), it can be observed that the hexagonal phase M (a continuous quaternary solid solution, formed between the ternary compound CuMgAl and the binary compound $MgZn_2$) is no longer present in the alloy structure and cubic phase Z (a continuous quaternary solid solution, between the ternary compound $Cu_6Mg_2Al_5$ and the binary compound Mg_2Zn_{11}) increases in concentration [25].

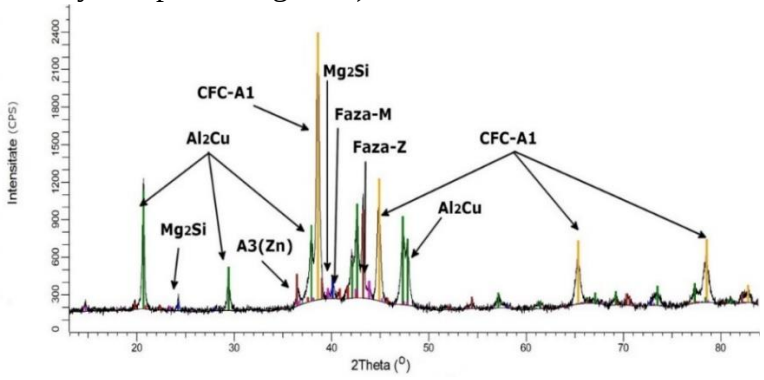

Figure 8.5. XRD diagram for as-cast $Al_{3.4}Cu_{0.5}Si_{0.2}Zn_{0.5}Mg_{0,2}$ alloy

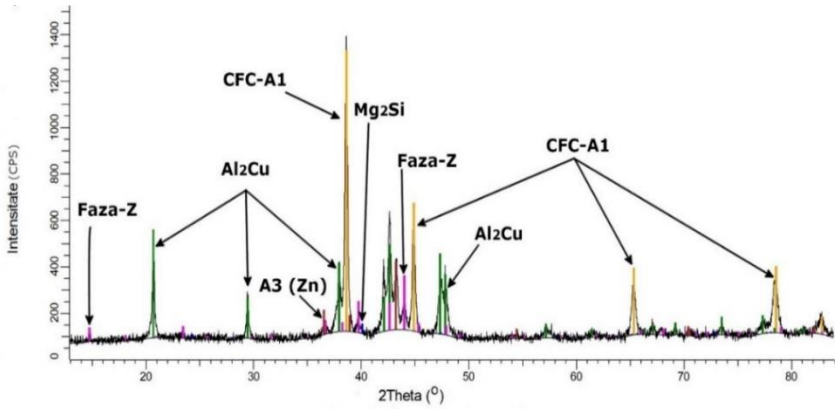

Figure 8.6. XRD diagram for annealed $Al_{3.4}Cu_{0.5}Si_{0.2}Zn_{0.5}Mg_{0.2}$ alloy

The XRD results of the $Al_5Cu_{0.5}Si_{0.2}Zn_{1.5}Mg_{0.2}$ alloy in the cast state (Fig. 8.7.) indicates a structure composed mainly of two solid solution phases (A1-Al) and (A3-Zn) and an intermetallic compound Al_2Cu. In addition to the complex and less stable compound $Mg_8Cu_2Al_4Si_7$, the compound Mg_2Zn_{11} was also detected in the as-cast alloy structure. The phases number of the alloy structure changed as a result of the heat treatment (Fig. 8.8.), where the formation of a phase with a high Si content can be identified.

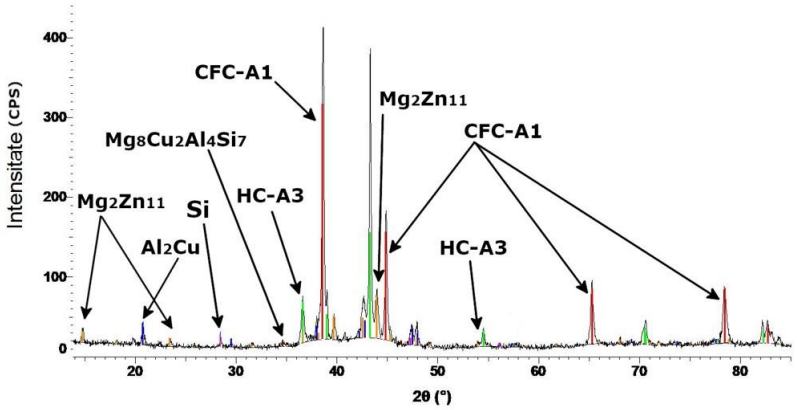

Figure 8.7. XRD diagram for as-cast $Al_5Cu_{0.5}Si_{0.2}Zn_{1.5}Mg_{0.2}$ alloy

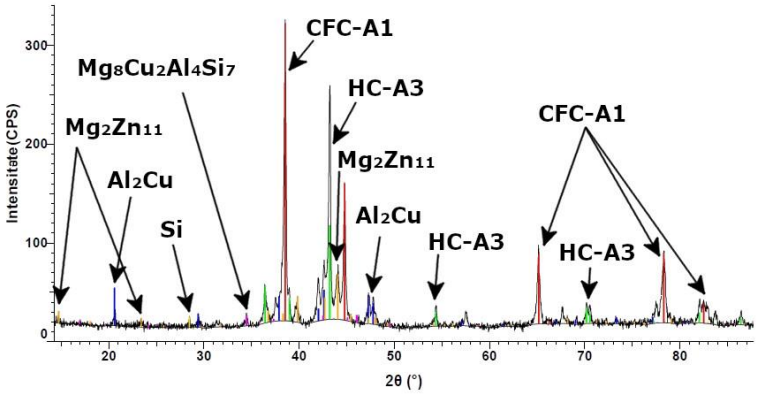

Figure 8.8. XRD diagram for annealed $Al_5Cu_{0.5}Si_{0.2}Zn_{1.5}Mg_{0.2}$ alloy

The as-cast state structure of the $Al_3Mn_{0.2}Si_{0.8}Zn_{0.3}Mg_{0.7}$ alloy (Fig. 8.9.) consists of solid solutions and intermetallic compound phases (CFC-Al (Al) solid solution type, intermetallic compounds $Al_{4.01}MnSi_{0.74}$, $Al_{10}(Mn_{0.58}Zn_{0.24}Si_{0.18})_3$, Mg_2Si and Si). $Al_{10}(Mn_{0.58}Zn_{0.24}Si_{0.18})_3$ is a hexagonal complex phase consisting of the binary compound $Al_{10}Mn_3$and the ternary compound $(Al_9Si)Mn_3$ (Fig. 8.10).

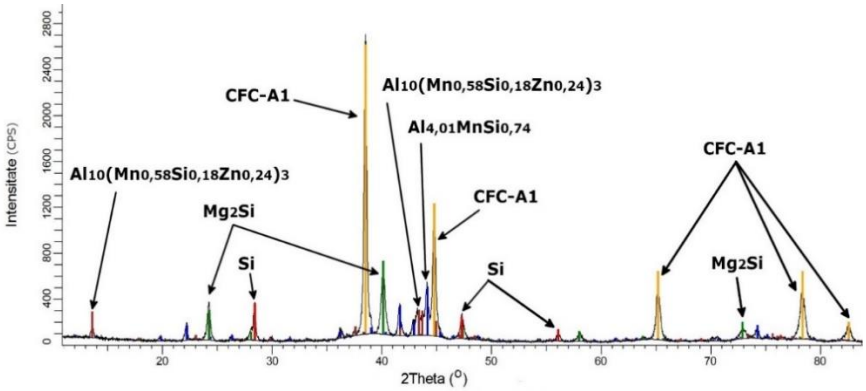

Figure 8.9. XRD diagram for as-cast $Al_3Mn_{0.2}Si_{0.8}Zn_{0.3}Mg_{0.7}$ alloy

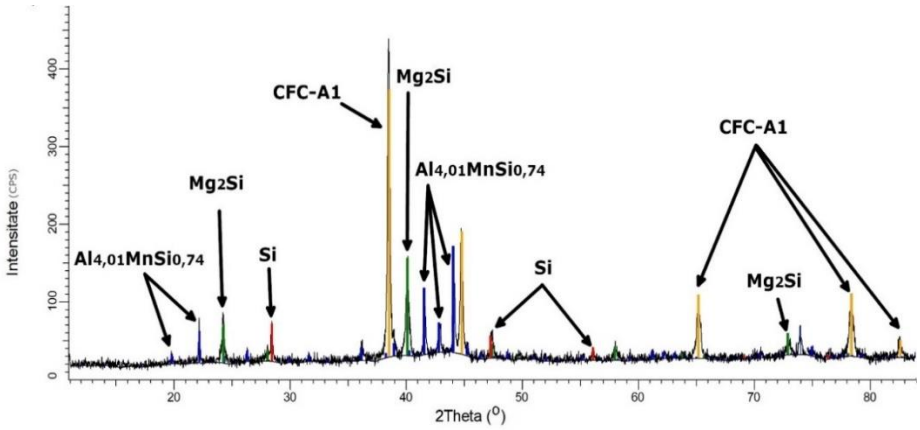

Figure 8.10. XRD diagram for annealed $Al_3Mn_{0.2}Si_{0.8}Zn_{0.3}Mg_{0.7}$ alloy

The X-ray diffraction analysis of the as-cast $Al_4Mn_{0.3}SiZn_{0.3}Mg$ alloy (Fig. 8.11.) identify a complex structure, consisting mainly of two solid solution phases (A1 based on Al) and (CC based on the ternary compound $Al_{4.01}MnSi_{0.74}$) and the intermetallic compound Mg_2Si. The annealed state $Al_4Mn_{0.3}SiZn_{0.3}Mg$ alloy diagram shows a crystal structure similar to the as-cast alloy state (Fig. 8.12).

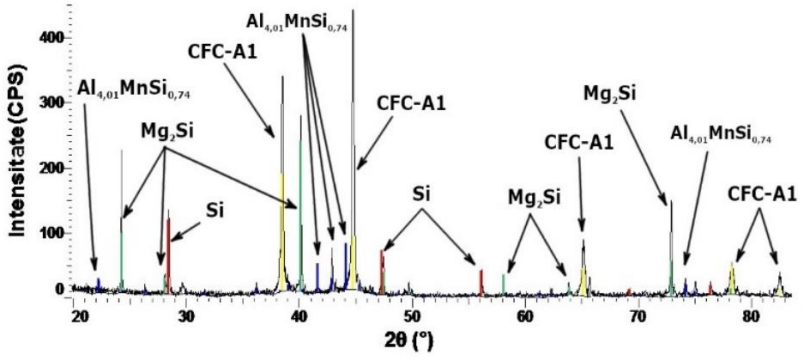

Figure 8.11. XRD diagram for as-cast $Al_4Mn_{0.3}SiZn_{0.3}Mg$ alloy

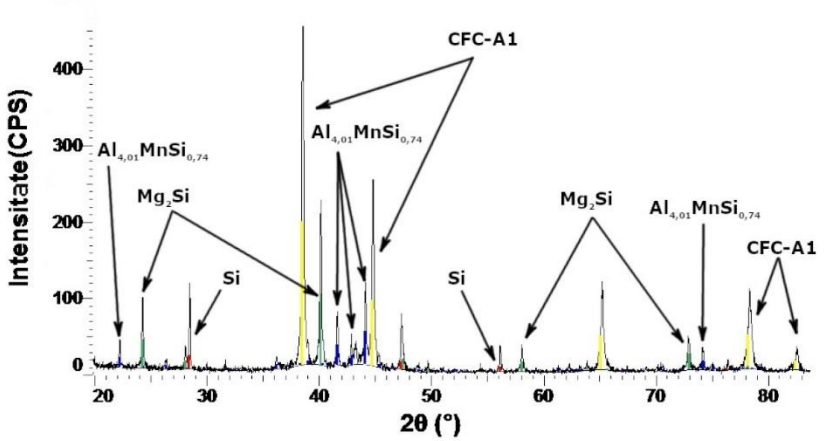

Figure 8.12. XRD diagram for annealed $Al_4Mn_{0.3}SiZn_{0.3}Mg$ alloy

8.2.4. Mechanical tests

The deformation slope of for the $Al_5Cu_{0.5}Si_{0.2}Zn_{1.5}Mg_{0.2}$ alloy has an ascending linear appearance in the plastic deformation range (Fig. 8.13). This continues with a downward failure curve around 800 MPa of compressive strength associated with a value of 0.04 corresponding to compressive stress. The material does not show a sudden or brittle rupture, which allows its use in various complex applications.

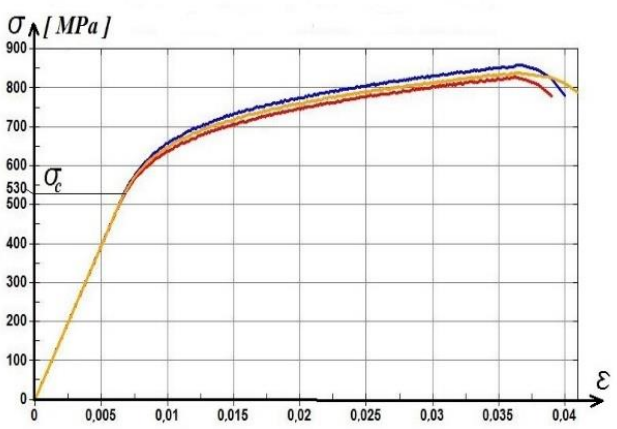

Figure.8.13. Strength-strain diagram of compression tests performed on as-cast $Al_5Cu_{0.5}Si_{0.2}Zn_{1.5}Mg_{0.2}$ alloy sample (σ—compression strength, σ_c—yield strength și ε—strain)

Microhardness tests showed high values compared to conventional aluminum alloys (A357.0 and AA5083) (fig. 8.14.).

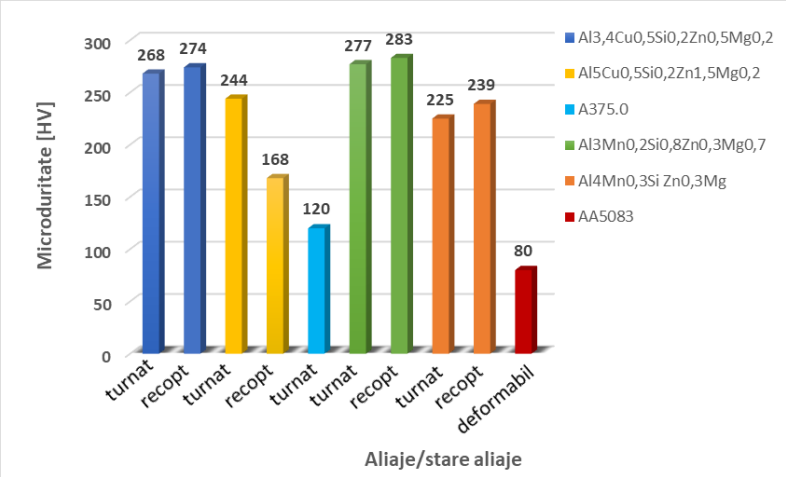

Figure 8.14. Graphical representation of the complex concentrated alloys microhardness compared to conventional aluminum alloys

CHAPTER 9. Characteristics of CCA alloy heat treated by quenching and aging

9.2. Characterization by scanning electron microscopy and energy dispersive spectrometry SEM -EDS

In all three samples (fig. 9.1), four phases were identified relatively uniform distributed in a matrix. Of these, three appear as plaques while the fourth is developed acicular. In the case of the alloy sample subjected to the aging treatment at 230°C for 50 hours, some phases form eutectic structures.

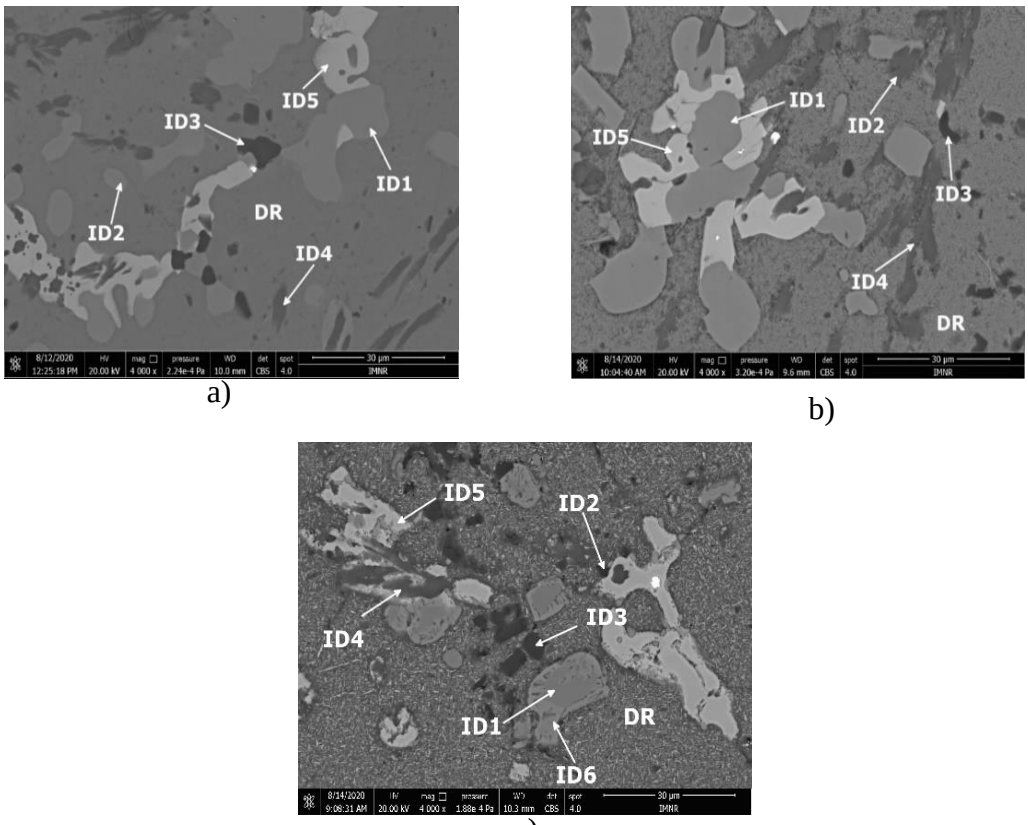

Figure 9.1. SEM image of $Al_5Cu_{0.5}Si_{0.2}Zn_{1.5}Mg_{0.2}$ alloy a) quenched, b) aged at 120 °C for 50 h and c) aged at 230 °C for 50 h

9.3. X-ray diffraction characterization of quenched and aged alloy

The X-ray analysis (Fig.9.2.) shows the phases that are formed in the $Al_5Cu_{0.5}Si_{0.2}Zn_{1.5}Mg_{0.2}$ alloy structure, as a result of the quenching treatment application. The alloy crystal structure is mainly composed of two solid solution phases (CFC-A1 and A3(Zn)) and the intermetallic compound Al_2Cu. In addition to these, the complex compounds $Mg_8Cu_2Al_4Si_7$ and Mg_2Zn_{11} with reduced stability can also be distinguished. Si is also identified as segregated in the alloy complex structure.

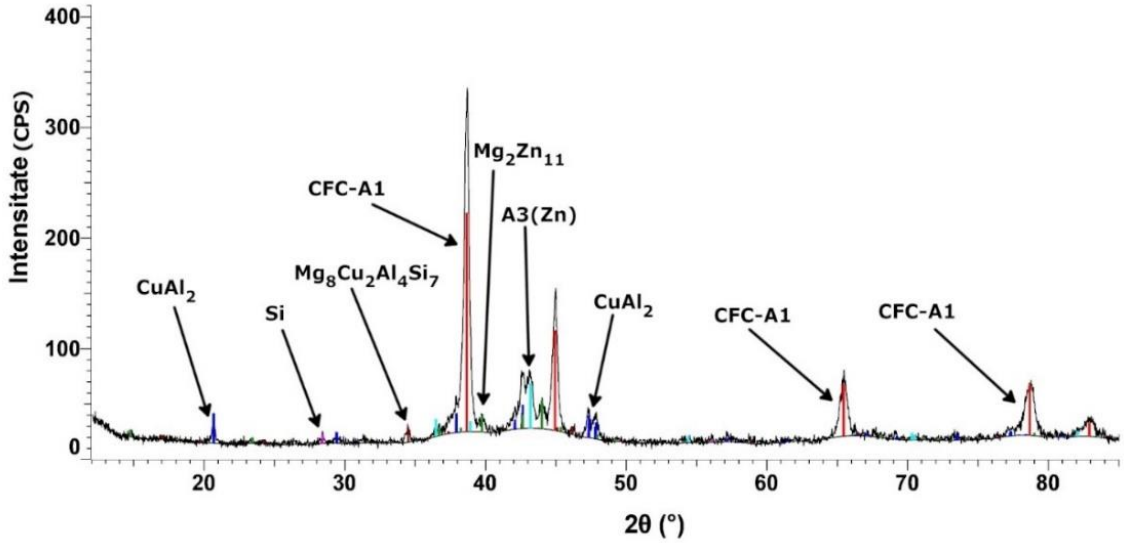

Figure 9.2. X-ray diffraction pattern of $Al_5Cu_{0.5}Si_{0.2}Zn_{1.5}Mg_{0.2}$ alloy in quenched condition

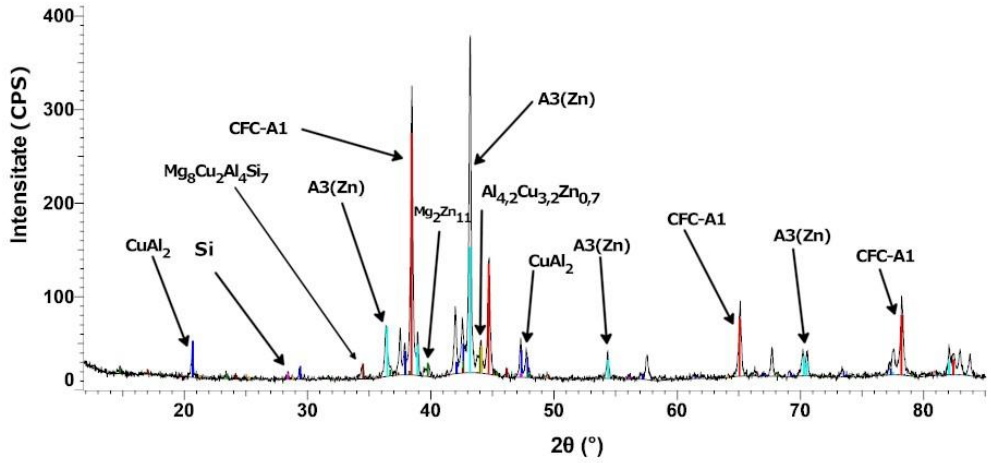

Figure 9.3. X-ray diffraction pattern of $Al_5Cu_{0.5}Si_{0.2}Zn_{1.5}Mg_{0.2}$ alloy aged at 120°C

For the $Al_5Cu_{0,5}Si_{0.2}Zn_{1.5}Mg_{0.2}$ complex concentrated alloy aged at 120°C and at 230°C, the x-ray analyzes (Fig. 9.3. and Fig. 9.4.) indicate an almost identical structure regarding the phases reported in the structure of the alloy in the quenching state. A major difference is determined by the aging treatment at 230°C which leads to the formation of the less stable $Al_{4.2}Cu_{3.2}Zn_{0.7}$ phase. At the same time, the A3(Zn) phase shows a more pronounced diffraction peak intensity for the alloy subjected to aging treatments compared to the alloy in the quenched state.

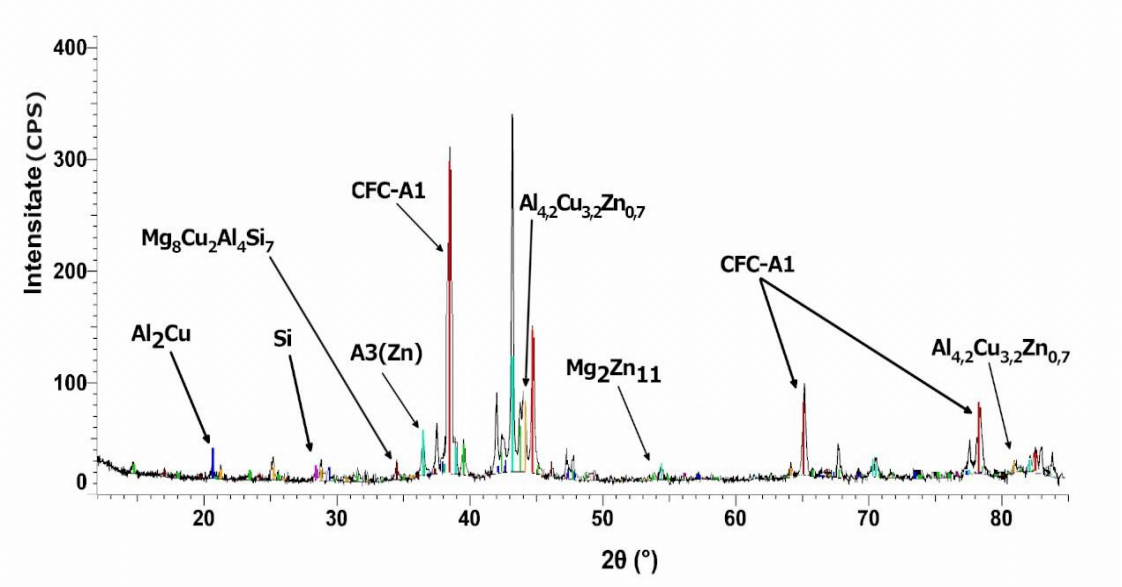

Figure 9.4. X-ray diffraction pattern of $Al_5Cu_{0.5}Si_{0.2}Zn_{1.5}Mg_{0.2}$ alloy aged at 230°C

9.4. Microhardness of quenched and aged alloy

The obtained samples after the thermal treatments applying were analyzed to determine the microhardness. The results are presented in table 9.1. and these indicate that the alloy sample subjected to the quenching treatment registers a lower value than the one obtained for the cast alloy and slightly superior to the aged alloy. The variation of the aging temperature did not greatly influence the microhardness of the alloy.

Table 9.1. Microhardness results for quenched and aged alloy

Alloy	Alloy state	Microhardness, [HV]
$Al_5Cu_{0.5}Si_{0.2}Zn_{1.5}Mg_{0.2}$	As-cast	238
	annealed	168
	quenched	192
	Aged (120°, 50 ore)	185
	Aged (230°, 50 ore)	181
316L	As-cast	178
A357.0	As-cast	120

The resulting alloy has a microhardness comparable to 316L stainless steel and higher than A375.0 cast aluminum alloy.

CHAPTER 10. Structural characterizations of the samples obtained through the rapid solidification process

The alloy ribbons have different thicknesses, with minimum and maximum values between 40-180 μm. Optical microscopy analysis (Fig. 10.1.) of the sample obtained at 500 rpm reveals a relatively coarse dendritic structure compared to the other ribbons. In the case of the other two samples (at 1000 rpm and 1500 rpm) optical microscopy highlights a fine inhomogeneous dendritic structure in the marginal area and a coarser one in the central area. In addition to the dendritic structure, two other phases and a eutectic developed in the interdendritic space were also identified in all three samples [26].

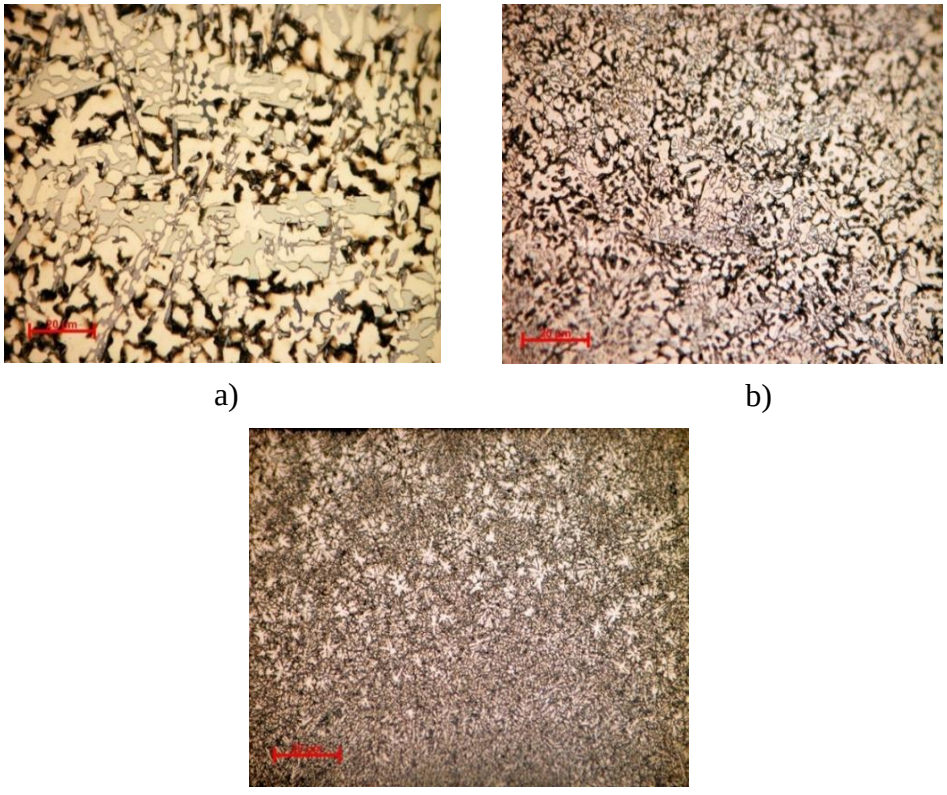

a) b)

c)

Figure 10.1. Optical microstructures of the alloy ribbons obtained at various speeds of the cooling disk (magnification 900X) a) 500 rpm b) 1000 rpm and c) 1500 rpm

The samples obtained at the crucible-disc distance of 0.5mm and 1mm investigated by optical microscopy show a very fine and homogeneous dendritic structure. This phenomenon is due to the high degree of alloy undercooling, which does not allow the sharp growth of dendritic phases (Fig. 10.2).

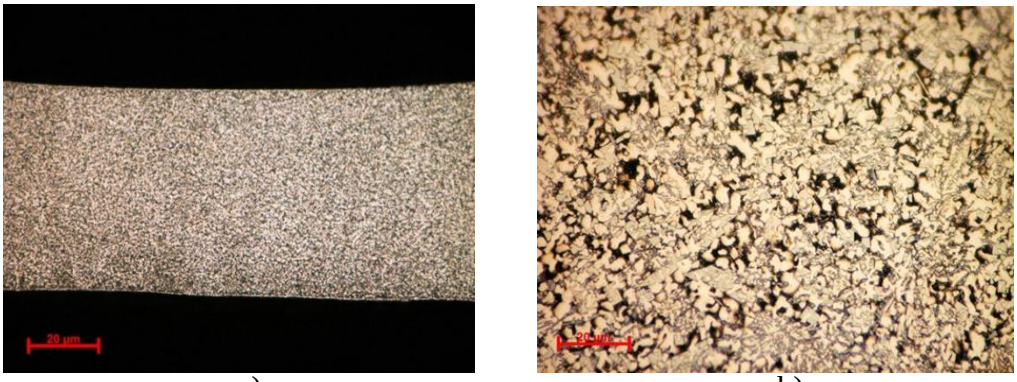

a) b)

Figure 10.2 Optical microstructures of the alloy ribbons obtained at various crucible-disc diameters (magnification 900X) a) 0.5 mm b) 1 mm

10.2. Characterization of alloy bands by scanning electron microscopy and SEM-EDS energy dispersive spectrometry

Scanning electron microscopy revealed that all samples have fine dendritic structures, the finer the higher number of rotations (fig. 10.3). The microstructure of all three analyzed samples is characterized by two main phases, one of which forms the dendrites, and the other phase is found in the interdendritic areas. It can be seen that the large number of rotations of the disk causes a fine dendritic structure of the bands, characterized only by the two main phases [26].

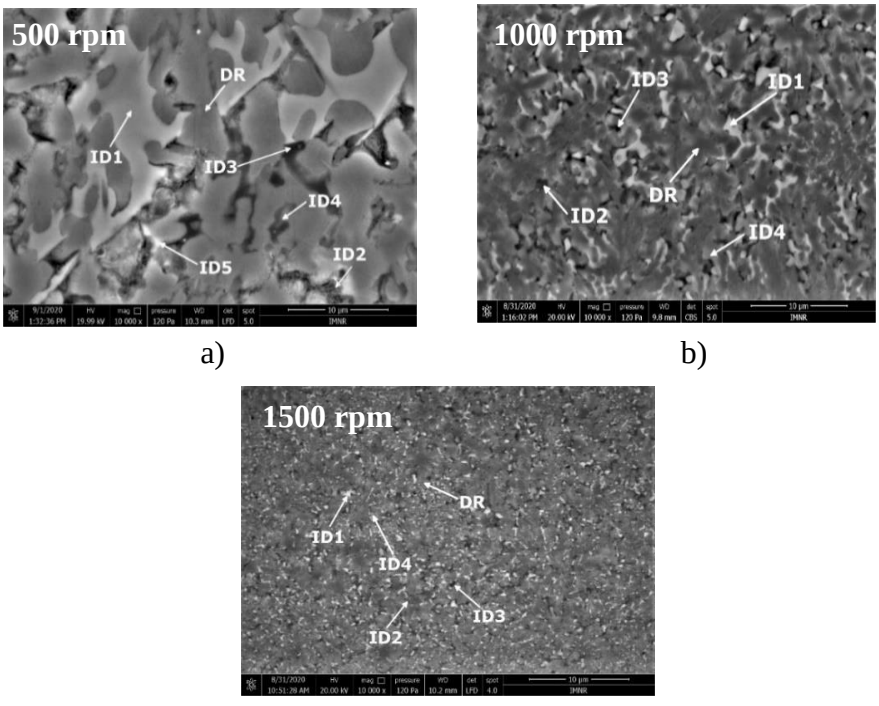

a) b)

c)

Figure 10.3. The microstructure of the ribbons obtained at various speeds of the cooling disk: a) 500 rpm (magnification 900X), b) 1000 rpm (magnification 900X) and c) 1500 rpm (magnification 900X).

The scanning electron microscopy images (Fig. 10.4.) reveal changes in the microstructure of the alloy ribbons, becoming finer as the distance between the crucible and the disc decreases. Thus, for the alloy ribbon obtained at a distance of 0.5 mm between the crucible and the disc, a very fine microstructure is highlighted, consisting only of a dendritic phase. As the distance between the crucible and the disc increases, another phase and a eutectic appear, both interdendritically located.

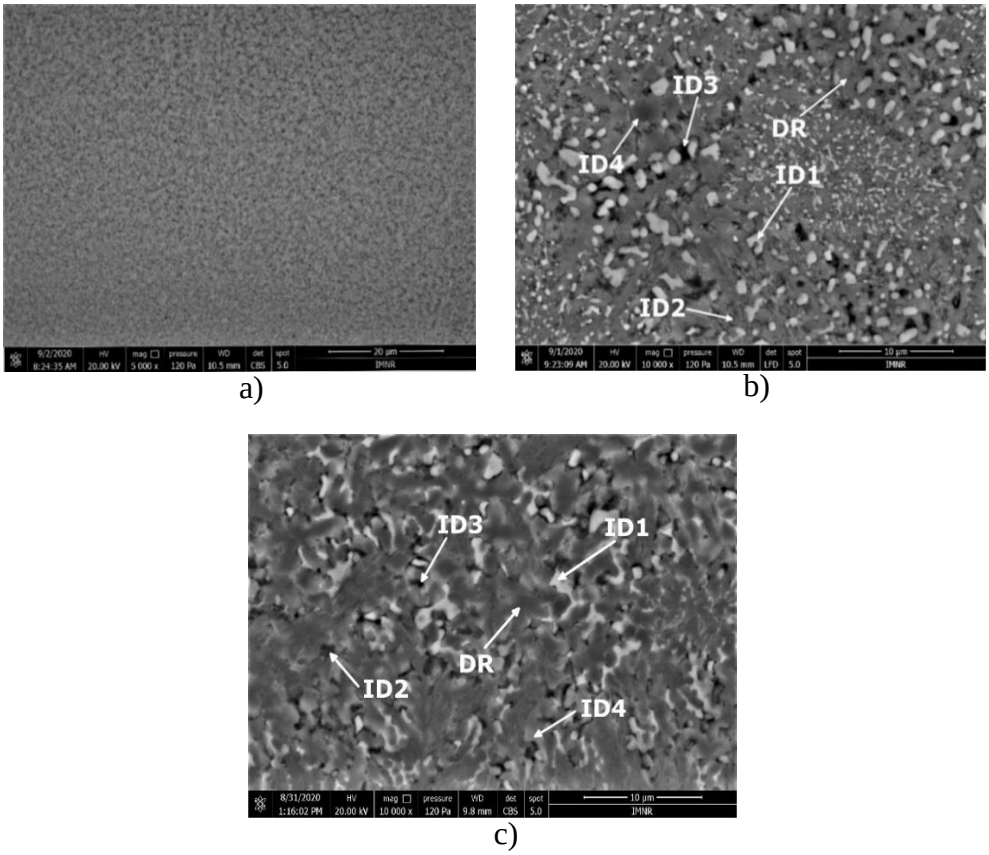

a) b)

c)

Figure 10.4. Microstructure of ribbons obtained at various crucible-disc distances: a) 0.5 mm (magnification 900X), b) 1 mm (magnification 900X) and c) 1.5 mm (magnification 900X).

10.3. Characterization of alloy ribbons by X-ray diffraction

X-ray analyzes of the rapidly solidified samples obtained at different disk rotation per minute (500 rpm, 1000 rpm and 1500 rpm) (fig. 10.5.) indicate similar structures. Thus, for the 3 types of samples, two solid solution-based structures are identified, whose composition includes Al and Zn (CFC-A1 and HC-A3) and the intermetallic compounds Al_2Cu, $Al_{4.2}Cu_{3.2}Zn_{0.7}$ and $Mg_8Cu_2Al_4Si_7$.

From fig. 10.6. the similarities of the crystalline structures of the alloy ribbons obtained by varying the crucible-disc distance parameter can be noted. The same 5 phases are identified for the 3 sample types, with Al and Zn as the main elements for two of the solid solution-based structures identified (CFC-A1 and HC-A3). At the same time, Al together with Cu, Zn, Mg and Si form three other intermetallic compounds Al_2Cu, $Al_{4.2}Cu_{3.2}Zn_{0.7}$ and $Mg_8Cu_2Al_4Si_7$. In

addition, the decrease in the intensity of the diffraction peaks characteristic of the Al_2Cu phase can be observed as the crucible-disc distance decreases.

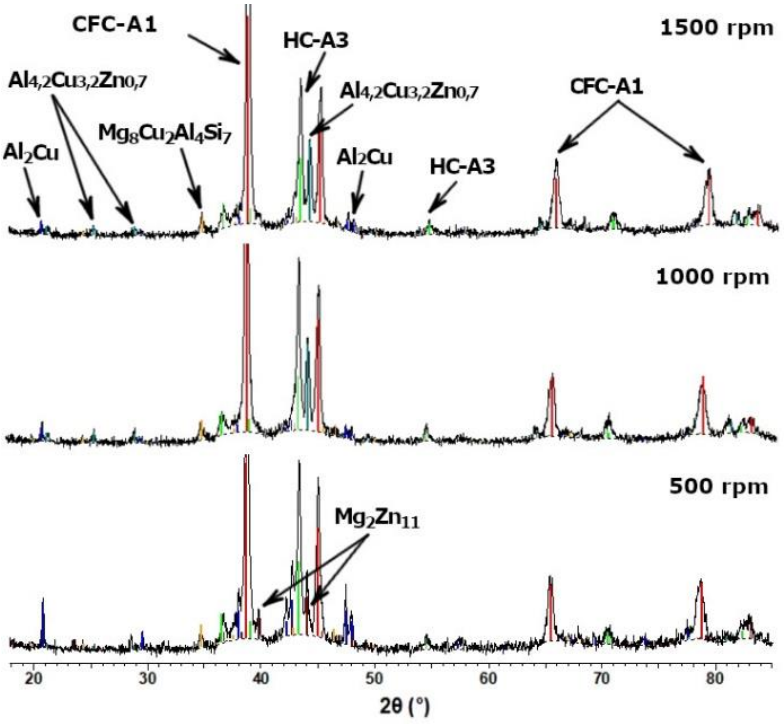

Figure 10.5. X-ray diffraction pattern of the alloy ribbons obtained at different disk rotation per minute (500 rpm, 1000 rpm and 1500 rpm)

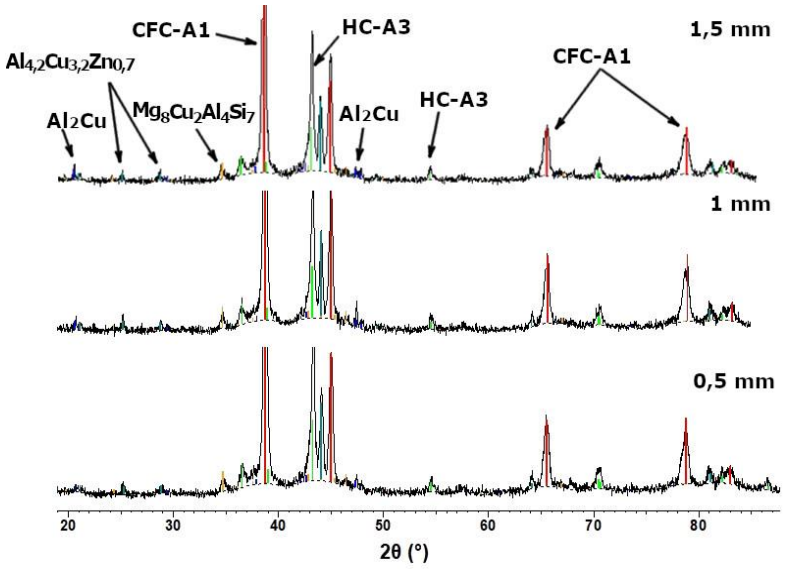

Figure 10.6. X-ray diffraction pattern of the alloy ribbons obtained at different distance between crucible and disk (0,5 mm, 1 mm and 1,5 mm)

CHAPTER 11. Corrosion resistance of $Al_5Cu_{0.5}Si_{0.2}Zn_{1.5}Mg_{0.2}$ alloy

The corrosion behavior was investigated for the $Al_5Cu_{0.5}Si_{0.2}Zn_{1.5}Mg_{0.2}$ alloy in the as-cast state and aging heat treatment at 230ºC temperature for 20 hours. Thus, the corrosion resistance of the alloy samples was analyzed by potentiodynamic polarization measurements (linear polarization resistance (LPR), Tafel diagrams (fig.11.1)) and electrochemical impedance

spectroscopy. Corrosion tests were performed in NaCl solution (3.5%). For comparison, the corrosion resistance of OL44 carbon steel was studied [24].

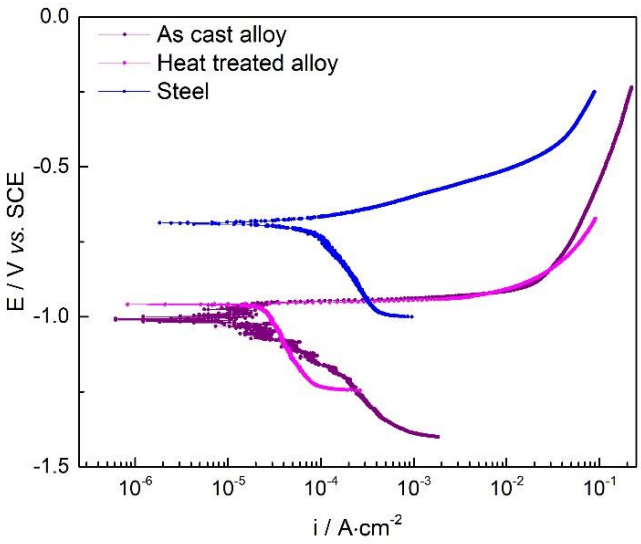

Figure 11.1. Tafel polarization curves for as-cast alloy, heat treated alloy and steel

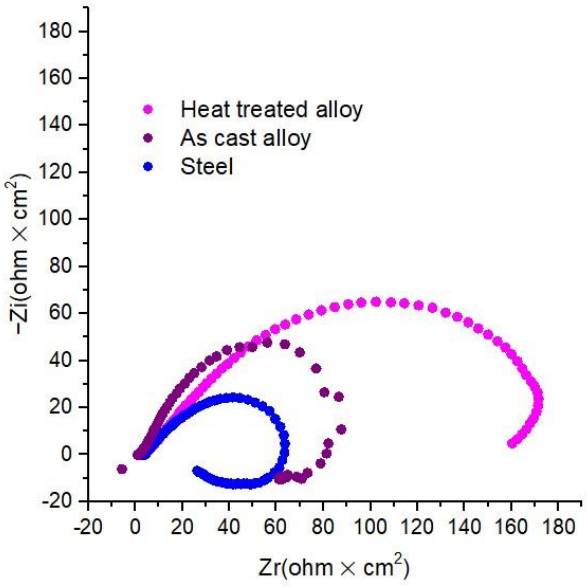

Figure 11.2. Nyquist diagrams for as-cast alloy, heat treated alloy and steel

Nyquist plots show (fig. 11.2) a capacitive loop correlated with the charge transfer process of corrosion compounds on the electrode surface. From the analysis of the samples impedance spectra, it can be seen that the diameter of the semicircles varies with the evolution of the corrosion process, due to the presence of the film composed of corrosion compounds.

Electrochemically, it is obvious that the Bode diagrams (fig.11.3.) indicate a single time constant, suitable for a well-established phase angle of approx. 38° for OL44, 47° for cast alloy and 58° for annealed alloy, which indicates that at high frequencies they have a capacitive behavior and at low frequencies they have an inductive behavior with low diffusive tendency.

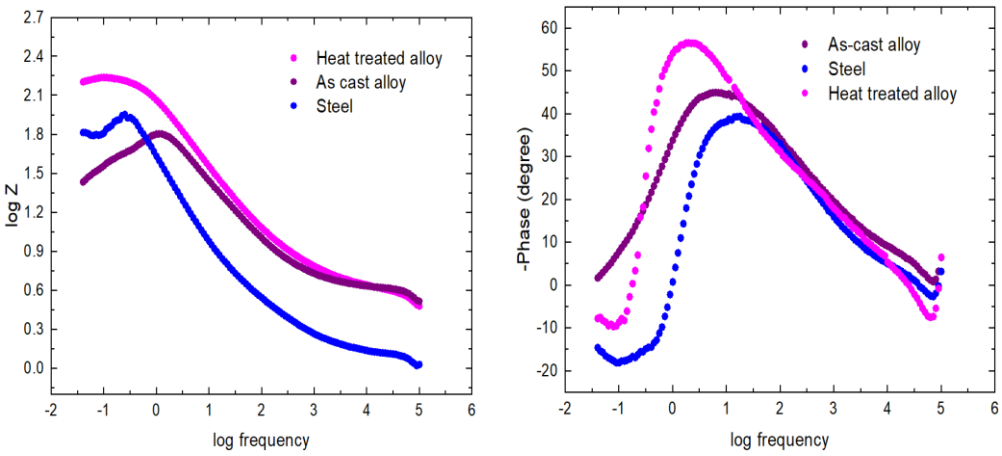

Figure 11.3. Bode diagrams for cast alloy, heat treated alloy and steel

The microstructural characterization results of the corroded films are presented in fig. 11.4 and fig.10.5. In general, an irregular structure with various phases having different morphologies can be noted. The corrosion layers examined on both samples appear to be partially fractured either due to fixation of the test chemical solution or due to the sample preparation process. There are no large cracks between the areas of the corrosion film. The appearance of the layers showed a significantly finer morphology for the annealed sample.

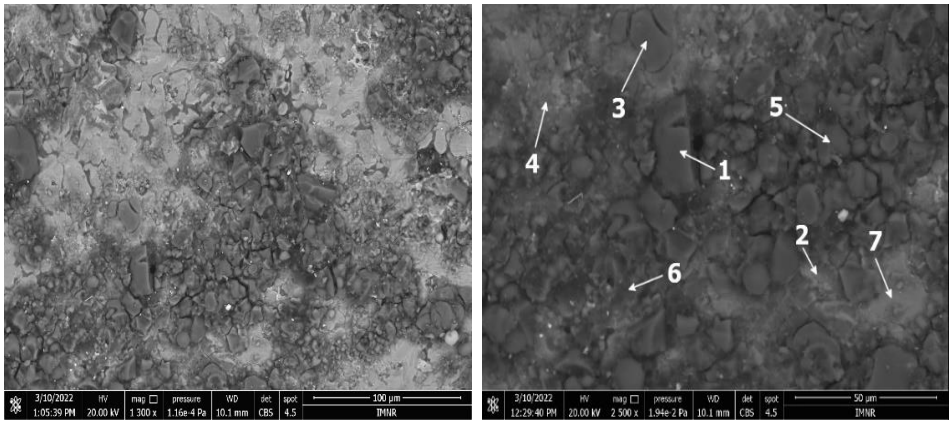

Figure 11.4. SEM images of the corroded surface of the as-cast alloy sample after the impedance tests. The marked areas were studied for EDS composition.

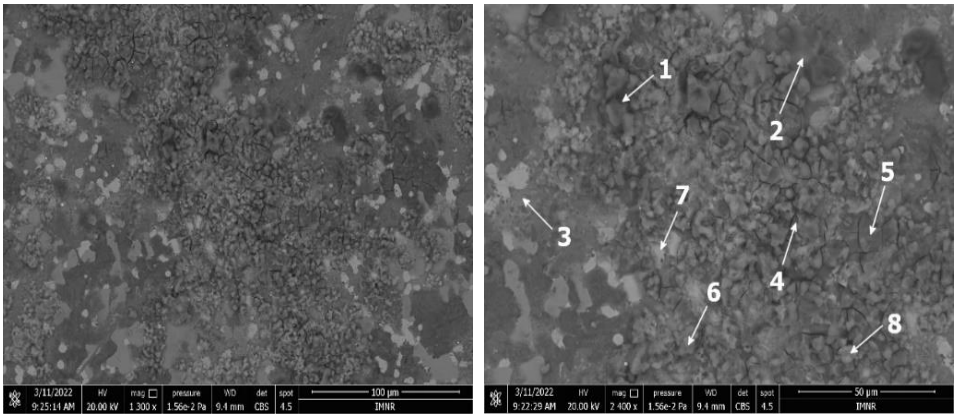

Figure 11.5. SEM images of the corroded surface of the heat treated alloy sample after the impedance tests. The marked areas were studied for EDS composition.

CHAPTER 13. Final conclusions, original contributions and future research directions

13.1. Final summary conclusions

Over time, the global trend of humanity has been oriented towards evolution, with the main objective being the improvement of living conditions. In this sense, the main tools of society were represented by metals, their alloys and the techniques of obtaining and processing. Nowadays, metallic materials play a significant role in most fields of activity and industries of interest, such as the maritime, aerospace, or construction industries. The current advances in materials engineering are due to structure of metallic materials advanced studies, their obtaining technologies, as well as their processing methods.

Complex concentrated alloys are considered a new category of multicomponent metallic materials, whose synthesis strategies are different from those of conventional alloys.

In this work, low-density complex concentrated alloys were developed, the characteristics of which include: superior oxidation and corrosion resistance, high hardness and wear resistance. They can be used in numerous applications, such as the car manufacturing industry (when making low-density parts), the naval industry (due to superior anti-corrosion characteristics), the aerospace industry (eg: the coupling pin manufacture or components that require low density and superior mechanical properties), etc.

In order to obtain the best compositions and characteristics, the selected alloy systems were subjected to thermodynamic and kinetic simulations (MatCalc - CALPHAD analysis technique) and multi-parametric modeling (Metalmix program).

The selection of alloys with low density and high solid solution content from Al-Cu-Si-Zn-Mg and Al-Mn-Zn-Mg-Si systems was performed by optimizing the previously established semi-empirical criteria. The results showed that a high aluminum content determined a better ability to form solid solution for both alloy systems, while Cu, Zn and Mn have a beneficial influence on the criteria parameters. On the other hand, elements increase content affects the density of the alloy. In the modeling performed with Metalmix software, the balance between density and optimal value criteria was considered in order to offer practical solutions in the selection process.

Selected alloys $Al_{3.4}Cu_{0,5}Si_{0.2}Zn_{0.5}Mg_{0.2}$, $Al_5Cu_{0.5}Si_{0.2}Zn_{1.5}Mg_{0.2}$, $Al_3Mn_{0.2}Zn_{0.3}Mg_{0.7}Si_{0.8}$ și $Al_4Mn_{0.3}SiZn_{0.3}Mg$ were analyzed for structural behavior using CALPHAD solidification and kinetics simulations. The phase diagrams showed the formation of mostly multiphase structures of solid solutions. Phases based on intermetallic compounds were identified at lower but still significantly higher concentrations than in conventional aluminum alloys. The influence of the elements on the structural evolution was similar to the results obtained from the semi-empirical criteria calculations. Non-equilibrium solidification simulation established the order in which the phases solidify under normal casting conditions. The CFC phase stabilizes first in the $Al_{3.4}Cu_{0.5}Si_{0.2}Zn_{0.5}Mg_{0.2}$ and $Al_5Cu_{0.5}Si_{0.2}Zn_{1.5}Mg_{0.2}$ alloys, while the Mg_2Si and Al_9Mn_2Si intermetallic compounds form first in the $Al_3Mn_{0.2}Zn_{0.3}Mg_{0.7}Si_{0.8}$ alloys and $Al_4Mn_{0.3}SiZn_{0.3}Mg$. Simulation of diffusion provided indications of the intermetallic precipitates formation in the solid solution matrix, showing that different phases stabilize at the highest concentration levels: Al_2Cu phase for $Al_{3.4}Cu_{0.5}Si_{0.2}Zn_{0.5}Mg_{0.2}$ and $Al_5Cu_{0.5}Si_{0.2}Zn_{1.5}Mg_{0.2}$, the Mg_2Si phase for the $Al_3Mn_{0.2}Zn_{0.3}Mg_{0.7}Si_{0.8}$ alloy and the AlCrFeMnSi phase ($Al_{4.01}MnSi_{0.74}$).

The modeling stage is an essential one, because it allows the compositions identification that best correspond to the desired applications, considering the degree of criticality of the component elements. Another advantage is the efficiency of the experimental stages, by

reducing the number of alloys obtained experimentally and, thus, reducing the costs related to material and energy consumption. Also, the mathematical simulation has the role of optimizing the compositions and processes of obtaining compositionally complex alloys, thus favoring the synergy between the properties and final destinations of the materials obtained.

The selected alloys compositions in the modeling stage were obtained experimentally using the induction melting furnace, which has the main advantages of achieving structural homogeneity, avoiding batch contamination, increased productivity and fast development time. They have a major impact on the materials used, substantially reducing the costs of obtaining, but also energy consumption, a fact that positively influences the ecological footprint of the process.

The materials obtained in the induction furnace were subjected to thermal treatments to improve the structure, which allow the reduction of internal stresses and obtaining a higher homogeneity.

Complex concentrated alloys, elaborated and heat treated, were characterized chemically, physically and structurally. The experimental results, provided by optical analysis, SEM-EDS and XRD, indicated complex structures of the alloys, mostly containing solid solutions, but also a significant amount of intermetallic phases. The Al-Cu-Si-Zn-Mg system alloys showed a refined structure in the as-cast state with a predominant dendritic phase containing a large proportion of Al. Most of the intermetallic phases of each individual alloy were also present in the alloy structure and continued to remain in a high percentage in the annealed sample. The exception is the hexagonal M phase which is present only in the cast structure of the $Al_{3.4}Cu_{0,5}Si_{0.2}Zn_{0.5}Mg_{0.2}$ alloy. The alloys from the Al-Mn-Zn-Mg-Si system presented a refined structure that was also maintained after the annealing treatment process application. This time, in the case of the two elaborated alloys, the dendritic formations were indicated to be the intermetallic phases: Mg2Si and $Al_{4.01}MnSi_{0.74}$. Between the as-cast and annealed states of the $Al_3Mn_{0.2}Zn_{0.3}Mg_{0.7}Si_{0.8}$ alloy, a less stable transformation of the compound $Al_{10}(Mn_{0.58}Zn_{0.24}Si_{0.18})_3$ into the compound $Al_{4.01}MnSi_{0.74}$ was determined, which led to a significant increase in its concentration.

Comparing the experimentally obtained results with the criteria calculations and the simulation results showed a good correlation. There are small differences regarding the phase composition and the behavior of the precipitating phases between the equilibrium diagrams made with CALPHAD for the alloys in both systems and differences between the kinetic simulation and the experimental results for the $Al_3Mn_{0.2}Zn_{0.3}Mg_{0.7}Si_{0.8}$ alloy.

Thermal analysis highlighted the main phase transformations that occur around 400°C for $Al_{3.4}Cu_{0.5}Si_{0.2}Zn_{0.5}Mg_{0.2}$ and $Al_5Cu_{0.5}Si_{0.2}Zn_{1.5}Mg_{0.2}$ alloys and around 500° C for $Al_3Mn_{0.2}Zn_{0.3}Mg_{0.7}Si_{0.8}$ and $Al_4Mn_{0.3}SiZn_{0.3}Mg$ alloys. The complex transformation that occurs in the $Al_5Cu_{0.5}Si_{0.2}Zn_{1.5}Mg_{0.2}$ alloy in the temperature range 400-500°C indicates a total or partial melting of the investigated sample.

The mechanical tests revealed that the microhardness of the analyzed alloys falls within the range of values for hard aluminum alloys (250–300 HV).

Due to the superior mechanical properties, low melting temperature and high thermal analysis temperature range that the $Al_5Cu_{0.5}Si_{0.2}Zn_{1.5}Mg_{0.2}$ alloy has, it was selected to be developed by a distinct synthesis method, using the rapid solidification facility. A reduction in the manufacturing costs related to the materials introduced and a reduction in the Mg content, considered a critical element, was observed, so a comparison between the two manufacturing methods of the alloy provides a wider perspective on the degree of correlation of the structure with the obtained properties. Also, the obtained alloy was subjected to complex thermal treatments of tempering and aging.

Rapid solidification experiments performed for the $Al_5Cu_{0.5}Si_{0.2}Zn_{1.5}Mg_{0.2}$ alloy indicated that the ribbons thickness is influenced by the distance between the crucible and the disk. The smaller the distance between disc crucibles, the lower the ribbons thickness. On the other hand, with increasing disc rotation, a decrease in ribbon thickness is observed. The samples obtained at 1500 rpm show the most pronounced degree of finishing. Microstructural analyzes highlighted the presence of very small grains with a dendritic shape and a uniform distribution of elements. It was found that the phase structures in the alloy bands are also confirmed by the previous microstructural analyzes for both the solidified and the heat treated alloy. In this sense, in order to obtain a fine grain and high homogeneity, it is recommended to develop the ribbons at high rotation speeds and small distances from the cooling disc.

The microstructural analyzes of the $Al_5Cu_{0.5}Si_{0.2}Zn_{1.5}Mg_{0.2}$ alloy subjected to heat treatments of quenching and aging show a uniform distribution of alloying elements in the material structure. Following the quenching process, the presence of smaller grains is observed compared to the as- cast alloy structure, while the aging treatment favors grain growth. SEM-EDS and DRX analyzes confirm small changes regarding the number of phases present in the alloy structure subjected to thermal treatments. The appearance of the $Al_{4.2}Cu_{3.2}Zn_{0,7}$ phase (t` phase) is influenced by the increase in the temperature of the aging treatment, remaining stable in the alloy structure. The efficiency of the aging heat treatment is demonstrated by the presence of the Al_2Cu type compound and its precipitation hardening in the solid solution mass.

Corrosion tests showed a relatively low corrosion rate value for the alloy in both the as-cast (0.3424 mm/year) and annealed (0.1972 mm/year) states. The passivation regions for both samples are formed late, at approx. 0.1 A/cm^2, which suggests the formation of a thin or penetrable oxide layer at the surface of the alloy. The best corrosion rate was obtained for the annealed alloy. Good corrosion resistance was also identified by impedance tests in heat-treated (6.5 ohm·cm^2) and as-cast (5.5 ohm·cm^2) samples. The inductive behavior present in the low frequency range is due to the relaxation process of some added species (corrosion compounds) at the surface of the working electrode. The data suggest that there is an adsorption process on the electrode surface. The results obtained from the EIS tests indicate that the charge transfer resistance Rct increased and the double layer capacity Cdl decreased with the strengthening of the layer formed by the anti-corrosion compounds.

The experimental results, correlated with the empirical ones obtained from the simulation processes, demonstrated an advanced potential of CCA alloys for use in multiple applications that require low density, superior mechanical characteristics and good resistance to oxidation and corrosion in extreme environments.

13.2. Personal, original contributions

The studies and research performed within the doctoral thesis, were aimed to develop new multicomponent materials, with improved properties, for multiple applications. The original character of the work is highlighted by:

- Carry out extensive documentary research on the technologies for the CCA alloys elaboration and the ways of obtaining superior properties;
- Application of the CALPHAD analysis method in the thermodynamic and kinetic processes simulation, but also of the structural transformations. Thus, the phases concentration of the analyzed alloy systems was determined, depending on the variation of the chemical elements. Equilibrium calculations, microstructural modeling and precipitation kinetics were also performed;
- In order to determine the optimal concentrations, the influence of the constituent elements on the materials structure was considered;

• Using induction field casting and rapid solidification technologies, new materials with multiple applications (marine industry, aerospace, etc.) were obtained;
• Annealing, quenching and aging heat treatments were applied to previously developed complex concentrated alloys. In this context, CCA alloys with low density and good resistance to oxidation and corrosion in extreme environments were obtained;
• The newly obtained multicomponent alloys were characterized physically, chemically, structurally, optically, XRD and electrochemically, using a previously established work plan.

13.3. Future directions for the development of doctoral thesis research

The research works presented in this doctoral thesis have not been studied at the national and international level, so they can be considered as a reference for further development directions. Considering the special properties that the newly developed CCA alloys have, it can be considered that they can successfully replace the traditionally used Al-based alloys in certain fields of interest.

The development of future research activities based on the doctoral topic addressed proposes the following perspectives:

• Investigating new methods of obtaining CCA alloys, such as thin films deposition;
• Development of new calculation models regarding the effect of slow diffusion, characteristic of complex alloys, which include reactive alloying elements;
• Multi-parametric optimization of the applied heat treatments, in order to obtain much improved mechanical properties, to expand the fields of applications;
• The future development of new research projects to stimulate the transfer of new knowledge acquired to industrial companies in the field.

DISSEMINATION OF THE RESULTS FROM THE DOCTORAL THESIS

Scientific publications during the doctoral stage (selection):

- Ioana Anasiei, Dumitru Mitrica, **Ioana-Cristina Badea***, Beatrice - Adriana Șerban, Johannes Trapp, Andreas Storz, Ioan Carcea, Mihai Tudor Olaru, Marian Burada, Nicolae Constantin, Alexandru Cristian Matei, Ana-Maria Julieta Popescu, Mihai Ghiță, Characterisation of complex alloys with potential in car brake manufacturing, Materials **2023**, Vol. 16 (14), 5067, https://doi.org/10.3390/ma16145067
- **Ioana - Cristina Badea**, Ioana Csaki, Beatrice - Adriana Șerban, Nicolae Constantin, Dumitru Mitrică, Marian Burada, Ioana Anasiei, Mihai Tudor Olaru, Andreea - Nicoleta Ghiță, Ana - Maria Julieta Popescu, Characterisation of a novel complex concentrated alloy for marine applications, Materials 2022, 15(9), 3345, https://doi.org/10.3390/ma15093345
- Beatrice-Adriana Serban, Mihai Tudor Olaru, **Ioana Cristina Badea***, Dumitru Mitrica, Marian Burada, Ioana Anasiei, Mihai Ghita, Ioan Albert Tudor, Cristian-Alexandru Matei, Ana Maria Julieta Popescu, Virgil Constantin, Florina Branzoi, Cristian Dobrescu, Nicolae Constantin, Non-Aqueous Electrodeposition and Characterization of AlCrCuFeNi High Entropy Alloy Thin Films, Materials 2022, 15(17), 6007; **https://doi.org/10.3390/ma15176007**
- D. Mitrica, **I. C. Badea***, B. A. Serban, M. T. Olaru, D. Vonica, M. Burada, R. R. Piticescu, V. Popov, „Complex concentrated alloys for substitution of critical raw materials in applications for extreme conditions", Materials 2021, *14* (5),1197;
- **https://doi.org/10.3390/ma14051197**
- B.A. Șerban**, I.C. Badea***, N.Constantin, D. Mitrică, M. T. Olaru, M. Burada, I. Anasiei,

S. E. Bejan, A.N. Ghiță, A. M. J. Popescu, Modeling and characterization of complex concentrated alloys with reduced content of critical raw materials, Materials 2021, Volume 14, Issue 18, 5263, https://doi.org/10.3390/ma14185263

- Ioana ANASIEI, **Ioana Cristina BADEA***, Beatrice Adriana SERBAN, Mihai Tudor OLARU, Denisa VONICA, Lidia LICU, Marian BURADA, Dumitru MITRICA, ”Researches regarding structural characteristics of a new complex concentrated alloy obtained by rapid solidification”, Proceedings 30th Anniversary International Conference on Metallurgy and Materials,p.1119-1124,2021, https://doi.org/10.37904/metal.2021.4225
- D. Mitrica, M. T. Olaru, V. Dragut, C. Predescu, A. Berbecaru, M. Ghita, I. Carcea, M. Burada, D. Dumitrescu, B. A. Carlan, **I. C. Banica** „Influence of composition and as-cast structure on the mechanical properties of selected high entropy alloys”, Materials Chemistry and Physics, 242, 2020, 122555, https://doi.org/10.1016/j.matchemphys.2019.122555
- M.Olaru, D. Mitrica, M. Burada, D. Dumitrescu, **C. Banica,** B. Carlan, D. Vonica, V. Dragut, V. Badilita, F. Stoiciu, Influence of heat treatment on $Al_{0.5}Cr_{0.5}Ni_{0.5}TiZr_{1.5}Nb_{1.5}$ high entropy alloy, U.P.B. Sci. Bull., Series B, Vol. 82, Iss. 2, 2020
- D. Mitrica**, I. C. Badea**, M. T. Olaru, B. A. Serban, D. Vonica, M. Burada, V. Geanta, A. N. Rotariu, F. Stoiciu, V. Badilita, L. Licu, Modeling and Experimental Results of Selected Lightweight Complex Concentrated Alloys, before and after Heat Treatment, Materials 2020, 13, 4330 **https://doi.org/10.3390/ma13194330**

National and international conferences (selection):

- **C. I. Banica**, D. Mitrica, M. T. Olaru, B. Carlan, D. Vonica, M. Burada, D. Dumitrescu, V. Geanta, I. Voiculescu, R. Stefanoiu, M. Ghita, V. Badilita, L. E. Barbulescu , L.Licu, Characteristics of low density high entropy alloys before and after heat treatment processing, 11th International Conference on Materials Science and Engineering – BraMat 2019, 13 – 16 Martie 2019, Brașov, Romania
- **C. I. Banica**, D. Mitrica, M. T. Olaru, B. A. Carlan, D. Vonica, L. Licu, M. Burada, D. Dumitrescu, V. Geanta, A. Rotariu, E. Scutelnicu, D. Savu, F. Stoiciu, V. D. Dragut, L.E. Barbulescu, Structure and properties of a new low weight high entropy alloy, EUROMAT2019, Stockholm, Suedia, 1-5 sept. 2019
- **C. I. Bănică**, D. Vonica, B. Șerban, L. Licu, M. T. Olaru, F. Stoiciu, V. Bădiliță, The design of a new low weight high entropy alloy, 2nd International Conference on Emerging Technologies in Materials Engineering, 6-8 Noiembrie 2019, Bucuresti, Romania
- **Cristina Ioana Badea**, Ioana Anasiei, Marian Burada, Dumitru Mitrica, Mihai Tudor Olaru, Beatrice Adriana Serban, Alexandru Matei, Ana Maria-Julieta Popescu, Virgil Constantin, Florina Brânzoi, Ionut Constantin, Irina Atkinson, Non-Aqueous electrodeposition and characterization of AlCrCuFeNi high entropy alloy thin films, Modern Technologies in Industrial Engineering-MODTECH 2022, 22-25 iunie 2022, Constanta, Romania.
- **Ioana-Cristina Badea**, Dumitru Mitrica, Ioana Anasiei, Beatrice Adriana Serban, Mihai Tudor Olaru, Marian Burada, Modelling process for multicomponent alloy selection with required application properties, Modern Technologies in Industrial Engineering-MODTECH 2022, 22-25 iunie 2022, Constanta, Romania.
- Beatrice Adriana Serban, Thomas Schubert, Andreas Storz, Ioana Anasiei, Marian Burada, Mihai Tudor Olaru, **Ioana Cristina Badea**, Johannes Trapp, Dumitru Mitrica, Andreea

Nicoleta Ghita, Alexandru Cristian Matei, Laura Eugenia Barbulescu, Characterisation of complex alloys with potential in car brake manufacturing, Modern Technologies in Industrial Engineering-MODTECH 2022, 22-25 iunie 2022, Constanta, Romania.

- I. Anasiei, D. Mitrică, M. Burada, B. A. Șerban, **I. C. Badea**, M. T. Olaru, S. A. Fironda, A. C. Matei, A. N. Ghiță, N. Vitan, J. Trapp, A. Storz, I. Carcea, New low weight complex concentrated alloy for high temperature applications, Emerging Technologies in Materials Engineering – EmergeMAT, 27-28 Octombrie 2022, Bucharest, Romania
- **Ioana Cristina Badea**, Beatrice Adriana Serban, Ioana Anasiei, Dumitru Mitrica, Mihai Olaru, Marian Burada, Adelina Ioana Matei, Mihai Ghita, Alexandra Gabriela Pascariu, Alexandru Cristian Matei, Structural behaviour of a low density high entropy alloys before and after heat treatment processing**,** Emerging Technologies in Materials Engineering – EmergeMAT, 27-28 Octombrie 2022, Bucharest, Romania

SELECTIVE REFERENCES

[1] D. B. Miracle, O. N. Senkov, „A critical review of high entropy alloys and related concepts," Acta Materialia, vol. 122, pp. 448-511, 2017.

[2] B. Cantor, I. T. H. Chang, P. Knight, A. J. B. Vincent, „Microstructural development in equiatomic multicomponent alloys," Materials Science and Engineering: A, Vol. 1 din 2375-377, pp. 213-218, 2004.

[3] J.-W. Yeh, S.-K. Chen, S.-J. Lin, J.-Y. Gan, T.-S. Chin, T.-T. Shun, C.-H. Tsau , S. -Y. Chang, „Nanostructured High-Entropy Alloys with Multiple Principal Elements: Novel Alloy Design Concepts and Outcomes," Advanced Engineering Materials, vol. 6, nr. 5, pp. 299-303, 2004.

[4] S. Ranganathan, „Alloyed pleasures: Multimetallic cocktails, Curr. Sci. 85," Current Science, vol. 85, nr. 5, pp. 1404-1406, 2003.

[5] D. B. Miracle, J. D. Miller, O. N. Senkov, C. Woodward, M. D. Uchic , J. Tiley, „Exploration and Development of High Entropy Alloys for Structural Applications," Entropy, vol. 16, nr. 1, pp. 494-525, 2014.

[6] D. B. Miracle, „Critical Assessment: Critical Assessment 14: High entropy alloys and their development as structural materials," Materials Science and Technology, vol. 31, nr. 10, pp. 1142-1147, 2015.

[7] C. Tiwary, V. V. Gunjal, D. Banerjee, K. Chattopadhyay, „Intermetallic eutectic alloys in the Ni-Al-Zr system with attractive high temperature properties," MATEC Web of Conferences, vol. 14, 2014.

[8] J.-W. Yeh, „ Recent Progress in High Entropy Alloys," Annales De Chimie – Science. des Materiaux, vol. 31, nr. 6, pp. 633-648, 2006.

[9] A. A. Gondhalekar, Design and Development of Light Weight High Entropy Alloys, School of Engineering, Jönköping University, 2019.

[10] B. S. Murty, J.-W. Yeh, S. Ranganathan, P. Bhattacharjee, High entropy alloys –2nd Edition, Elsevier, 2019.

[11] Y. Zhang, Y. J. Zhou, J. P. Lin, G. L. Chen, P. K. Liaw, „Solid-solution phase formation rules for multi-component alloys," Advanced Engineering Materials, vol. 10, p. 534–538, 2008.

[12] W. Hume-Rothery, Atomic Theory for Students of Metallurgy, London: The institute of Metals, 1969.

[13] W. Hume-Rothery, H. M. Powell, „On the theory of super-lattice structures in alloys," Zeitschrift für Kristallographie - Crystalline Materials, pp. 23-47, 1935.

[14] W. Hume-Rothery, R. W. Smallman, C. W. Haworth, The structure of the metals and alloys, London: The Institute of Metals, 1969.
[15] S. Guo, C. Ng, J. Lu, C. T. Liu, „Effect of valence electron concentration on stability of FCC or BCC phase in high entropy alloys," Journal of Applied Physics, vol. 109, 2011.
[16] S. Guo, C. T. Liu, „Phase selection rules for complex multi-component alloys with equiatomic or close-to-equiatomic compositions," Chinese Journal of Nature, vol. 35, nr. 2, pp. 85-96, 2013.
[17] S. Guo, „Phase selection rules for cast high entropy alloys: an overview," Materials science & technology, vol. 31, pp. 1223-1230, 2015.
[18] O. N. Senkov, D. B. Miracle, „A new thermodynamic parameter to predict formation of solid solution or intermetallic phases in high entropy alloys," Journal of Alloys and Compounds, vol. 658, pp. 603-607, 2016.
[19] I. H. Jung, M.-A. Van Ende, „Computational Thermodynamic Calculations: FactSage from CALPHAD Thermodynamic Database to Virtual Process Simulation," Metallurgical and Materials Transactions B, vol. 51, p. 1851–1874, 2020.
[20] A. C. Chang, S. Chen, F. Zhang, X. Yan, X. F., R. Schmid-Fetzer, W. A. Oates, „Phase diagram calculation: Past, present and future," Progress in Materials Science, vol. 49, nr. 3-4, pp. 313-345, 2004.
[21] K. C. Chou, Y. A. Chang, „A Study of Ternary Geometrical Models," Berichte der Bunsengesellschaft für physikalische Chemie, vol. 93, pp. 735-741, 1989.
[22] S. Gorsse, J. Couzinié, D. Miracle, „From high-entropy alloys to complex concentrated alloys," Comptes Rendus Physique, vol. 19, nr. 8, pp. 721-736, 2018.
[23] M. A. Fentahun, M. A. Savaş, „Materials Used in Automotive Manufacture and Material Selection Using Ashby Charts," International Journal of Materials Engineering, vol. 8, nr. 3, pp. 40-54, 2018.
[24] **I.-C. Badea**, I. Csaki, B.-A. Serban, N. Constantin, D. Mitrica, M. Burada, I. Anasiei, M. T. Olaru, A.-N.Ghita, A.-M. J. Popescu, „Characterisation of a novel complex concentrated alloy for marine applications," Materials, vol. 15, nr. 9, 2022.
[25] D. Mitrica, **I. C. Badea**, M. Olaru, B. Serban, V. D. Olaru, M. Burada, V. Geanta, A. Rotariu, F. Stoiciu, V. Badilita , L. Licu, „Modeling and experimental results of selected lightweight complex concentrated alloys, before and after heat treatment," Materials, vol. 13, nr. 4330, 2020.
[26] I. Anasiei, **I. C. Badea**, B. A. Serban, M. Olaru, D. Vonica, L. Licu, M. Burada , D. Mitrica, „Researches regarding structural characteristics of a new complex concentrated alloy obtained by rapid solidification," Proceedings 30th Anniversary International Conference on Metallurgy and Materials, pp. 1119-1124, 2021.